FINITE-AMPLITUDE STANDING WAVES IN RIGID-WALLED TUBES

WAYNE L. BEECH

FINITE-AMPLITUDE STANDING WAVES

IN RIGID-WALLED TUBES

by

Wayne "L" Beech
Commander, United States Navy
B.S.E.E., Georgia Institute of Technology, 1953

Submitted in partial fulfillment of the
requirement for the degree of

MASTER OF SCIENCE IN PHYSICS

from the

NAVAL POSTGRADUATE SCHOOL
December 1967

ABSTRACT

Finite-amplitude standing wave effects in air at ambient conditions contained in rigid-walled cylindrical tubes with large length to diameter ratios were experimentally investigated. These results were compared to a perturbation solution of the one-dimensional non-linear acoustic wave equation which incorporates the dissipative effects due to viscous and thermal energy losses at the walls. The lowest resonance frequencies of the tubes ranged from 62.5 Hz to 1 kHz, and sound pressure levels (based on the fundamental) ranged up to 160 dB. The finite-amplitude distortion was in excellent agreement almost up to the onset of shock. A detailed investigation of small amplitude attenuation in standing wave tubes was conducted and compared with the Kirchhoff equations. Agreement within one percent was obtained when consideration was given to the numerical analysis correction and end-effect losses.

TABLE OF CONTENTS

LIST OF TABLES

LIST OF ILLUSTRATIONS

LIST OF ILLUSTRATIONS (continued)

LIST OF SYMBOLS

a = Lagrangian coordinate measured from piston

A = instantaneous acceleration of piston

A_o = (peak) acceleration amplitude of piston

B/A = parameter of nonlinearity $= \rho_o (d^2_\rho p)/(d_\rho p)$ at $\rho = \rho_o$

c = phase velocity in the tube

$c_o = (dp/d\rho)^{\frac{1}{2}}$ at $\rho = \rho_o$

$k = \omega/c$

$k = k - i\alpha$

$K = m\pi/L$

L = Lagrangian coordinate of rigid end of tube

m = denotes normal mode of tube most strongly excited by input frequency

$M = U_{11}/c_o$ = peak Mach number of first-order solution

p, p_o = acoustic pressure, equilibrium pressure

P_{nj} = jth frequency component of the nth order perturbation pressure

P = (infinitesimal) pressure amplitude at the rigid end of the tube

P_{nj} = amplitude of P_{nj}

Q_n = resonance parameter (see Eq. 38)

$Q_n(M, \Delta\omega)$ = The normalized magnitude of the Q-Curve for the nth harmonic using the perturbation solution

$Q_n'(M, \Delta\omega)$ = The normalized magnitude of the Q-Curve for the nth harmonic using the Fourier synthesis solution

$S_A = V_A/A_o$ = accelerometer sensitivity

$S_M = V_M/P$ = microphone sensitivity

u = particle velocity

u_n = particle velocity of the nth order perturbation solution

u_{nj} = jth frequency component of u_n

V_A = (peak) amplitude of voltage output of accelerometer

V_M = (peak) amplitude of voltage output of microphone

α = infinitesimal-amplitude attenuation constant

α_{cal} = calculated tube attenuation with Shield's correction but not including end effects

α_e = attenuation due to end losses (see Eq. 51)

α_{exp} = experimentally determined attenuation

α_t = wall attenuation using Weston's equation (see Eq. 41)

α_T = total calculated attenuation (see Eq. 47)

α_w = wall attenuation using Kirchhoff's equation (see Eq. 48)

β = $1 + \frac{1}{2}(B/A)$

γ = c_p/c_v = ratio of specific heats

γ' = Kirchhoff's constant (see Eq. 42)

δ = dissipation parameter (see Eq. 13)

δ_j = value of δ for (angular) frequency ω_j

θ_n = phase parameter

ξ = particle displacement

ρ/ρ_o = instantaneous density, equilibrium density

ϕ_n = forcing term (see Eq. 39)

ω = $2\pi f$ = (angular) driving frequency

ω_r = infinitesimal-amplitude resonance frequency

$\Delta\omega$ = $\omega - \omega_r$

D = $(\rho_o c_o^2)^{-1} \partial_t F$

D_j = D for frequency ω_j

F = operator for body forces

$\Box^2$ = $\partial_a^2 - c_o^{-2} \partial_t^2$ = D'Alambertian in Lagrangian coordinates (one spatial dimension)

ACKNOWLEDGEMENT

The encouragement and advice of Professors James V. Sanders and Alan B. Coppens is gratefully acknowledged.

Thanks are also due Mr. William E. Smith for his assistance in fabricating parts of the experimental setup.

1. Introduction

It has been known for a long time that for the case of a plane elastic wave of any amplitude in a nondissipative medium the exact solution to the equations of hydrodynamics predicts a change in form as the wave travels (1,2,3,4,5,6). In going one step further and considering that the medium is dissipative, it can be shown that only waves of relatively large amplitude evidence any appreciable change in form (4,7). This provides a good definition for finite-amplitude waves. Stated another way, a wave would be of finite-amplitude when the inclusion of second-order terms are required for the theory to predict a change in shape as the wave propagates.

An important contribution beyond the work done by the early investigators of the nineteenth century was by Fay (8). He investigated the change of type in a periodic finite-amplitude plane wave of infinite extent in a viscous medium. He formed a Fourier-series solution valid far from the source that was an attenuated saw-tooth wave.

In general the more recent theoretical approaches to finite-amplitude effects have been of two types. Approximation methods using some assumption on the manner of harmonic generation and absorption in a medium have been used (9,10,11,12), and approximate solutions to the nonlinear differential equations by the perturbation technique or other means have been investigated (8,13,14,15,16).

An expression for the spatial attenuation of an plane saw-tooth wave finite in extent was developed by Rudnick (17,18) using a "first-order" theory. Since the wave was confined, consideration was given to the attenuation due to the walls by using the results of Kirchhoff and Helmholtz.

Goldberg (13,14) undertook a solution of the problem of plane waves in an unbounded medium by a direct perturbation approach on the equations of motion. He obtained a number of second-order solutions and was able to provide conclusions about the relative importance of nonlinearity and dissipation.

The perturbation analysis has been extended to the sixth order by Keck and Beyer (15) for periodic plane progressive waves of infinite extent in a viscous medium. The wave equation is the same one treated by Fay, but the solution is valid near the source.

A numerical solution for approximately the same problem has been obtained by Cook (20). An exact solution in parametric form was obtained by Blackstock (21) for the problem of a finite-amplitude sound wave produced by arbitrary motion of a piston in a lossless tube.

Most investigators, like the ones already discussed, have confined their studies to traveling waves. However, a few have given consideration to standing waves.

An exact solution of the nonlinear wave equation for the case of finite-amplitude standing waves in a closed tube as well as for one having a vibrating piston at one end was obtained by Keller (22). Upon assigning a value of -1 to the adiabatic exponent γ, the nonlinear wave equation becomes linear, and this fact was used by Keller in his solution. These results "blow-up" at resonance because the dissipative forces are neglected in the solution.

Betchov (23) constructs a solution at resonance based on discontinuous linearized solutions and a secular equation. This solution is interesting in that for an invisid fluid the amplitude at resonance is found to be finite and to be determined by non-linear effects. Betchov also discusses

the modifying effect of wall friction on his solution and assumes that this effect is equivalent to a body force proportional to the velocity.

Saenger and Hudson (24) present a simple analytical description of the behavior of periodic shocks at resonance using a two part solution of the nonlinear one-dimensional wave equation. A point of importance in their solution is that the amplitude of the oscillations remains finite only because of the action of shear viscosity and heat conduction.

Chester (25) has predicted asymmetries in finite amplitude standing waves with an elaborate theoretical investigation based on the nonlinear acoustic equations. The solution includes the effects of compressive viscosity, and of shear viscosity in the boundary layer at the walls of the tube; however, his solutions are not amenable to detailed experimental comparison.

Coppens and Sanders (26) developed an extension of Keck-Beyer perturbation approach that included both the bulk losses and the wall losses. Their results provide information on the amplitudes and phases of the Fourier components of the distorted pressure waveform. The theory is applied to the problem of finite-amplitude standing waves in a cylindrical resonance tube that is excited by a piston at one end. This perturbation approach was extended by Ruff (27), and computer programs were written to extract more information from the theory.

The purpose of this research was to conduct a detailed experimental investigation of finite-amplitude standing waves in air contained in rigid-walled tubes to verify the soundness of the

Coppens-Sanders theory as extended by Ruff. In addition, a detailed investigation of the attenuation of sound in rigid-walled standing wave tubes with attention given to end-effect losses was conducted to check the validity of applying the Kirchhoff attenuation equations to standing waves.

2. Theory

2.1 General

A plane elastic wave traveling in a fluid exhibits a change in form as it travels. This can be seen from the nonlinear properties of the equations of state and motion which follow. This theoretical development is extracted from that of Coppens and Sanders and is presented here to aid in interpreting the experimental work.

The adiabatic equation of state of a fluid

$$(p+p_0)/p_0 = (\rho/\rho_0)^{\gamma} \tag{1}$$

can be represented by a truncated Taylor's expansion in the form

$$p = (A/\rho_0)(\rho-\rho_0) + (B/2\rho_0^2)(\rho-\rho_0)^2 \tag{2}$$

where

p = acoustic pressure

ρ = instantaneous density at a point

ρ_0 = equilibrium density

B/A = parameter of nonlinearity.

If the fluid is an ideal gas, then B/A = γ -1 where γ is the ratio of principal specific heats. The coefficient A can be expressed as

$$A = \rho_0 c_0^2 \tag{3}$$

where

c_0 = infinitesimal amplitude free field phase velocity.

The equation of continuity for one dimensional wave propagation can be written in Lagrangian coordinates as

$$\rho(1+\partial_a \xi) = \rho_0 \tag{4}$$

where ξ is the particle displacement from the initial position at a.

The force equation can be written in a slightly generalized form as

$$\rho_0 \partial_t u = -\partial_a p + \mathcal{F}_L u \tag{5}$$

when $u = \partial_t \xi$ is the particle velocity and the operator F_L generates those body forces in Lagrangian form that are active in the system of interest.

The combination of Eqs. 2-5 yields

$$\partial_t^2 \xi - c_0^2 (1+\partial_a \xi)^{-2} \left[1 - (B/A)\partial_a \xi (1+\partial_a \xi)^{-1}\right] \partial_a^2 \xi = \rho^{-1} \mathcal{F} u \tag{6}$$

which for an ideal gas becomes

$$\partial_t^2 \xi - c_0^2 (1+\partial_a \xi)^{-\gamma-1} \partial_a \xi = \rho^{-1} \mathcal{F} u . \tag{7}$$

For acoustic processes where $\partial_a \xi << 1$, Eq. 7 can be approximated by

$$\Box_L^2 \xi + (\rho_0 c_0^2)^{-1} \mathcal{F} \partial_t \xi \doteq \beta \partial_a (\partial_a \xi)^2 \tag{8}$$

Differentiation of Eq. 8 with respect to time yields

$$(\Box_L^2 + \mathcal{D}_L) u \doteq \beta \partial_a \partial_t (\partial_a \xi)^2 \tag{9}$$

where

$$\begin{aligned} \beta &= 1 + \tfrac{1}{2}(B/A) \\ \mathcal{D}_L u &= (\rho_0 c_0^2)^{-1} \partial_t \mathcal{F} u \\ \Box_L^2 &= \partial_a^2 - c_0^{-2} \partial_t^2 \end{aligned} \tag{10}$$

Equations 6-9 have been the basis of a number of theoretical investigations utilizing successive approximations or perturbation expansions to describe finite-amplitude effects for traveling waves in fluids (with or without viscous dissipation) (8,9,10,15,21,28).

Under the assumption of weak dissipative processes and with the substitution of the perturbation series $\xi = \sum_m \xi_m$, Eq. 9 becomes

$$\sum_j (\Box_L^2 + \alpha Q_j) v_{mj} = \phi_m \tag{11}$$

where the sum over j is understood to encompass just those frequencies appearing in ϕ_m with

$$\phi_m = \beta \partial_x^2 \alpha_3 \sum_{j=1}^{m-1} \alpha_j \xi_j \partial_x \xi_{m-j} \qquad m > 1 \tag{11a}$$

$$\phi_m = 0 \qquad m = 1 . \tag{11b}$$

To predict the finite-amplitude effects for one-dimensional wave propagation in a fluid system, it is only necessary to obtain the linearized, absorptive wave equation for the system, substitute the resulting expression for D_u into Eq. 11, and solve for the frequency components.

2.2 Rigid-Walled Tubes

Weston's (29) approach to the propagation of sound waves in gases contained in wide tubes can be used in the formulation of D_u. For the wide tube the sound energy is diffused evenly over the tube cross section, and the adiabatic motion approximates to that in an unbounded gas. There is, however, a narrow boundary layer at the wall, analogous to the Prandtl boundary layer in continuous flow, where viscous and heat conduction processes lead to an energy loss. The losses in the boundary layer at the wall are much greater than the bulk losses. Weston's equation in Eulerian form can be written as

$$\Box_E^2 u + \delta(\omega - i)\partial_x^2 u = 0 \tag{12}$$

where

$$\delta = (\sigma/S)(2\omega)^{-\frac{1}{2}} \tag{13}$$

$$\gamma' = \gamma^{1/2} + (\gamma - 1)(\nu'/\nu)^{1/2} \quad = \text{Kirchhoff's constant} \qquad (14)$$

S = (uniform) cross-sectional area

G = perimeter of area S

ω = (angular) frequency of the propagating waveform

ν = kinematic shear viscosity of the fluid

ν' = thermal diffusivity or thermometric conductivity

$i = \sqrt{-1}$.

The real part of $\underset{\sim}{u}$ represents the mainstream particle velocity in the tube. For Eq. 12 to be valid $\ell \ll S^{1/2}$ where ℓ is the boundary layer thickness given approximately by $5(\nu/\omega)^{\frac{1}{2}}$ (29). Equation 12 can be written as

$$\Box_E^2 u + (\delta/\omega)\partial_x^2 \partial_t u - \delta \partial_x^2 u = 0 \qquad (15)$$

with the assumption of one-dimensional flow.

Then

$$\Box_j^2 = (\delta_j/\omega_j)\partial_x^2 \partial_t - \delta_j \partial_x^2 \qquad (16)$$

where δ_j represents the value of the dissipation parameter δ for a frequency ω_j.

The approximate wave equation is now given by

$$\prod_j \left(\Box^2 + \frac{\delta_j}{\omega_j}\frac{\partial^3}{\partial x^2 \partial t} - \delta_j \frac{\partial^2}{\partial x^2}\right) u_m = \beta \frac{\partial^2}{\partial a \partial t} \sum_{i=1}^{n-1} \frac{\partial \xi_i}{\partial a} \frac{\partial \xi_{m-1}}{\partial a} = \phi_m = \sum_j \phi_{mj} \qquad (17)$$

For a resonance tube of uniform cylindrical cross-section excited at a = 0 by a piston with the same cross sectional area driven with constant acceleration at an angular frequency ω and terminated at a = L by a plane rigid boundary, the appropriate boundary conditions can be written as

$$u_m(0,t) = (A_1/\omega)\sin(\omega t - \Theta_1) \qquad (18)$$

$$u_{n1}(L,t) = u_{n2}(0,t) = u_{n2}(L,t) = 0 \qquad n > 1. \tag{19}$$

The phase angle θ_j will be specified later. From these boundary conditions Coppens and Sanders present a solution that describes the finite-amplitude waveform. Certain quantities developed by Coppens and Sanders are important in any experimental investigation and are therefore reproduced here. The propagation constant, k, and the small amplitude attenuation constant, α, are given by

$$k = \omega/c \doteq (\omega/c_0)(1 + \tfrac{1}{2}\delta_1) \tag{20}$$

and

$$\alpha \doteq (\omega/c_0)(\tfrac{1}{2}\delta_1). \tag{21}$$

α will be discussed in greater detail in Section 3.3.

Various frequency relationships in terms of the infinitesimal-amplitude resonance frequency, ω_{r0}, are given by

$$\Delta\omega = \omega - \omega_{r0} \tag{22}$$

for the frequency differential from resonance and

$$\omega_4 = \omega_{r0}(1 + \tfrac{1}{2}\delta_1) \tag{23}$$

for the frequency at which each harmonic making up the pressure waveform has decreased in value to $1/\sqrt{2}$ of its maximum value. The dissipation parameter for higher order, δ_m, is given by

$$\delta_n = \delta_1 / n^{1/2} \tag{24}$$

where the integer n represents the harmonic. It is also convenient to introduce the peak Mach number of the first-order solution

$$M = U_{11}/c_0 \tag{25}$$

3. Experimental Considerations

Insight into the finite-amplitude case can be gained by first relating the theory to the infinitesimal-amplitude case with a view toward isolating the experimentally determinable parameters. From the expressions

$$U_{II} = (A_0/\omega)(\sinh^2 \alpha L + \sin^2 kL)^{-1/2} \tag{26}$$

and

$$p = \rho c_0 U_{II} e^{i(\omega t - \pi/2)}, \tag{27}$$

the pressure at the rigid end of the tube can be found to be

$$p_1(L,t) = (\rho c_0 A_0/\omega)(\sinh^2 \alpha L + \sin^2 kL)^{-1/2} \sin \omega t. \tag{28}$$

When the acceleration of the piston is written as

$$A(0,t) = A_0 \sin(\omega t + 90° - \theta_1), \tag{29}$$

it can be seen that the piston leads the first-order pressure at the rigid end of the tube by $90^\circ - \theta_1$. The first-order pressure amplitude at the rigid end when the attenuation is small can be written as

$$P_{II} \doteq (\rho c_0 A_0/\omega)\left[(\alpha L)^2 + \sin^2 kL\right]^{-1/2}, \tag{30}$$

and the phase angle θ_1 becomes

$$\tan \theta_1 = (\tan kL)/(\alpha L) \tag{31}$$

At resonance Eqs. 30 and 31 become

$$P_{II} = \rho c_0 A_0/\alpha \, \pi L \tag{32}$$

and

$$\theta_1 \doteq 0 \tag{33}$$

where the integer m represents the normal mode most strongly excited by the input frequency. When finite-amplitude effects are taken into consideration, the pressure is modified by the presence of the higher harmonics and can be written as

$$P(L,t) \doteq P_{11}\sin\omega t + P_{22}\sin(2\omega t+\theta_2) + P_{33}\sin(3\omega t+\theta_3+\theta_3)+\cdots . \quad (34)$$

It is convenient to introduce the resonance parameter Q_n and the phase parameter θ_n defined by

$$Q_m = \pm (\cos\theta_m)/\delta_m \quad (35)$$

and

$$\tan\theta_m = (\delta_1 - \delta_m - 2\Delta\omega/\omega_1)/\delta_m , \quad (36)$$

The dependence on the small amplitude attenuation coefficient α is best introduced at this point by writing the dissipation parameter δ_m in the form

$$\delta_m = 2\alpha c_0/\omega m^{1/2} \quad (37)$$

through the use of Eqs. 24 and 21.

If Q_n and θ_n are rewritten in terms of α, under the assumption that the bulk losses are less than the boundary layer losses, then the approximate forms are given by

$$Q_m \doteq m^{1/2}\omega\cos\theta_m/4\alpha c_0 \quad (38)$$

and

$$\tan\theta_m \doteq 1/m^{1/2} - m^{1/2}\Delta\omega/\alpha c_0 . \quad (39)$$

For a resonance tube with a diameter of 1.125 inches, a length of 6 feet, and a fundamental resonance frequency of approximately 100 Hz, the bulk losses do not equal the boundary layer losses until the input frequency is of the order of 10^6 Hz. This would be in the range of

the 10^4 harmonic, and it is readily seen that the assumption that the boundary layer losses dominate is valid.

Equations 26-39 can be readily used for a comparison with the theory. The factors $\beta, \rho_o,$ and c_o are known for the system to be used, and the quantities A_o and $\omega(2\pi f)$ are known input variables. α, ρ_o and c_o can be determined experimentally. The pressure amplitude P_{nn} can be measured directly, and θ_n can be determined from the frequency dependence of the pressure measurements.

Examination of certain of these terms reveals some important properties. Q_n is maximum above ω_{p_n} and the higher the subscript n the higher the maximizing frequency. With constant acceleration, the higher harmonics have their maximum amplitudes at successively higher frequencies with narrower peaking, and the frequency region for most favorable finite-amplitude excitation lies between ω_p and $\omega_1 = \omega_p(c_o/c)$. The angle θ_n describes the difference in phase between the piston acceleration at a = o and the pressure at a = L.

3.1. System and Equipment Description

A diagram of the system used in this experimental investigation is shown in Fig. 1. The resonance tubes contained air at ambient temperature and pressure. In order to insure as nearly as possible ideal boundary conditions and to reduce the effects of mechanical coupling with the exciter, the resonance tubes were fabricated of steel with an inside diameter of 2.250 inches and a wall thickness of 1.125 inches. The inside surface of the tube wall was cleaned, but no other attempt was made to improve the finish. The rigid end was terminated with an aluminum cap 2.0 inches thick. To insure no leaks, the surface of the cap and the end of the tube was machined

and polished and high vacuum silicone grease was used as a sealer. The cap was held in place by five studs screwed into the tube wall. A total of five tubes (identical except for length) were used to give a spread in fundamental resonant frequencies in excess of an order of magnitude. The lengths of the tubes were 7, 14, and 28 inches and 6 and 9 feet. The six foot tube was used for the major portion of the investigation and for comparison with the computer predicted results.

The piston design was critical for several reasons. It had to be heavy enough that a minimum of distortion was introduced by the force exerted upon it by the distorted standing wave, yet light enough that desired acceleration amplitudes could be obtained. A piston weight of approximately 0.8 pounds was used. A clearance of approximately 0.006 inch was provided between the seat and the piston, and an air-tight seal was obtained by the use of two O-rings and silicone grease. The O-ring grooves in the piston were designed so that the neoprene O-ring would be under compression and were spaced to provide a reservoir for the grease. A smooth seat for the piston was provided by machining and grinding the inside of the tube. The plane surface of the piston was machined and polished.

The M-B Electronics Model EA 1500 exciter due to its versitility, small size, and maximum acceleration rating of 124 g's was chosen as the acoustic driver. For the production of intense standing waves in a resonance tube, large displacement amplitudes are not needed, but large acceleration amplitudes are needed. The permanent magnet vibration generator with its large force ratings and small moving mass readily meets these requirements. The frequency and amplitude

can be varied simply by adjusting the oscillator output. The EA 1500 has a frequency range from 5 Hz to 10 kHz which is well beyond the first cross mode of operation and the limiting value for this investigation.

The M-B Electronics model 2120MB power amplifier was selected to complement the exciter. The distortion was less than 0.7% at rated output of 125 watts in the desired frequency range of operation and less than 0.3% at driving levels below shock. A single unit provided accelerations to 50g's for the piston used. Higher levels of acceleration can be obtained by paralleling additional power amplifiers.

The severe requirements for a very highly stable oscillator with a precisely repeatable frequency setting led to the choice of the General Radio Type 1161A-A6C coherent decade frequency synthesizer as the primary frequency source. The synthesizer has a readily repeatable frequency setting to better than 0.001 Hz. The synthesizer was checked repeatedly with a counter, and no variation in the frequency output was measured. The output level control was modified to permit finer adjustment. A General Radio Type 1160-P2 Sweep and Marker generator was used in conjunction with the synthesizer.

The piston motion was monitored by the use of a Endevco model 2215 accelerometer mounted inside the piston. This model will work directly into a VTVM and still provide satisfactory frequency response up to 10 kHz. It was necessary to mount the accelerometer on the centerline of the piston and directly to the leading component of the piston to reduce distortion and improve the accuracy of the results.

The Hewlett-Packard Electronic Counter Model 521C was used to monitor the frequency input and the frequencies from the wave analyzer.

No deviations were noted between the set frequency and the output frequency for the synthesizer.

A Bruel and Kjaer Type 4136 condenser microphone was mounted in the rigid end so that the diaphragm was flush with the end of the tube. T he small diameter (only ¼ in.) was chosen to minimize the disturbance of the rigid boundary condition. The frequency response of the microphone was flat to within ± 0.5 dB from 80 Hz to 20 kHz, well beyond the range of interest for all five tubes. The rise time of this microphone was 4.5 microseconds.

All voltage measurements were taken with Hewlett-Packard 400D Vacuum tube voltmeters, and the waves shapes were observed using a Tektronic Type 565 dual-beam dual-trace oscilloscope. The distortion present in the wave forms was analyzed for harmonic content using a General Radio Type 1900-A wave analyzer. This analyzer has a band width selection of 3, 10, and 50 Hz. Some Q-curves were plotted using data Equipment Company Model 800 AM X-Y recorder and the General Radio sweep and marker generator.

Figure 2 is a schematic of the system used to monitor the temperature of the gas. Because of its linear resistance characteristic in the range of interest, a Fenwal Electronics Inc. Model GA 51P1 thermistor was used and was mounted in a small hole drilled in the rigid end plate. The leads were insulated, and the unit was set in epoxy with the glass bead at the surface. The epoxy provided an excellent seal and a means of smoothing the end plate to reduce distortion. The temperature read-out was provided by means of a microammeter; when a continuous record was needed, a strip recorder

was used. The system was calibrated with the aid of temperature baths of acetone and dry ice, ice and water, and boiling water. With this system, temperature changes in the tube of less than 0.1 C^{o} could be easily detected.

3.2. Calibration of Equipment

The experimental determination of P_{nn} requires that the absolute calibrations of the microphone be known. In addition, the determination of α requires that the absolute calibration of the accelerometer also be known. The accelerometer sensitivity is defined as $S_A = V_A/A_o$ where V_A is the peak amplitude of the accelerometer output voltage, and the microphone sensitivity is defined as $S_M = V_M/P$ where V_M and P are the peak amplitudes of the microphone output voltage and the pressure respectively.

The calibration of the accelerometer was accomplished by direct measurement of the displacement amplitude of the piston face for a range of accelerometer output voltages. Displacement amplitudes up to 0.060 cm were measured with a reproducibility of 0.0002 cm using a traveling microscope and a stroboscopic light. At 100 Hz, fifteen determinations of the accelerometer sensitivity resulted in $S_A = (6.66 \pm 0.03) \times 10^{-4}$ volt/(m/sec^2).

The microphone was calibrated using a Bruel and Kjaer Model 4220 pistonphone which produces a known acoustic pressure level of 124 $\pm$ 0.2 dB at a frequency of 250 Hz. The sensitivity was found to be $S_M = (-76.4 \pm 0.2)$dB re volt/μb = $(1.50 \pm 0.03) \times 10^{-3}$ volt/(Nt/m^2).

3.3. Determination of the Attenuation Constant

The necessity of having an accurately determined small amplitude attenuation coefficient and the reported wide variation in agreement between the theoretical and the experimentally determined attenuation, particularly in tubes containing standing waves, prompted a more thorough investigation of this problem.

3.3.1. Background

Beginning with Helmholtz in 1863 (30), who considered only the effects due to viscosity, the causes of the sound attenuation in cylindrical tubes have been widely discussed and investigated (29,31-42). Experiments of Kundt led to Kirchhoff's (6) complete theory for the wide tube (defined in Section 2.2) which considered both viscosity and heat conduction. In general, investigators report that the Kirchhoff equation gives the proper frequency, radius, and pressure dependence but that the experimental absorption is greater than calculated. Weston (29) presented more accurate expressions for the velocity and attenuation by including more terms in the expansion of the Bessel functions. Weston's expressions for velocity and attenuation for the wide tube (which we are considering) are:

Phase velocity of sound:

$$c' = c\left[1 - \frac{\gamma'}{r_0}\left(\frac{2\omega}{}\right)^{1/2}\right] \qquad (40)$$

$$= 3.434 \times 10^4 \left[1 - 0.162 \cdot (r_0\sqrt{f})\right] \quad \text{cm-sec}^{-1}$$

Attenuation:

$$\alpha_{tr} = \frac{\gamma'}{r_0 c}(\omega/2)^{1/2} + \frac{\omega^2}{2c^3}\left[2 + \gamma' + \frac{\gamma - 1}{\gamma}\gamma'\right] + \frac{\omega^2 \gamma'^2}{4c^2} \qquad (41)$$

$$= \left[2.904 \times 10^{-5}/r_0 + 1.403 \times 10^{-13} f^2 + 0.806 \times 10^{-3}\right] \text{cm}^{-1}$$

where

$$\gamma' = \sqrt{\gamma} + (\gamma - 1)(\gamma/\gamma)^{1/2} = 0.574 \text{ cm/sec}^{1/2} \quad (42)$$

The first term of Eq. 41 is the ordinary wall absorption, the second the ordinary free gas attenuation, and the third arises because the sound energy is not uniformly distributed over the tube. The numerical values here are for dry air a 20°C and 760 mmHg and were checked using constants obtained from National Bureau of Standards Circular 564 (43).

Shields, Lee and Wiley (44) present a numerical solution of the Kirchhoff equation and state that Kirchhoff's phase velocity correction is always too large (giving values which are too small), and that the calculated absorption is always too small. They also give a method for determining the error in the Helmholtz-Kirchhoff equations.

The work thus far presented is for progressive waves in infinitely long tubes. It has been stated by Shields (44) that neither the Kirchhoff tube absorption and velocity equations nor the numerical analysis would be expected to apply to standing wave tubes.

In considering resonance tubes, there is almost universal agreement on the existence of excess experimental absorption (44-48) when compared with the absorption calculated using the equations for traveling waves. For example, Parker (45) reported an excess which varied from 6.5% for helium to 30% for argon; Smith and Tempest (44) report 30%; Henderson and Donnelly (46) found 10%.

3.3.2. Theory for Standing Waves

For standing waves to be generated in a rigid-walled tube, an integral number of half wave lengths must be contained in the tube length, i.e., $\lambda_m = 2L/m$ where m = 1,2,3,... From the fact that

$\lambda_m = c/f_m$:

$$f_m = m(c/2L) \tag{43}$$

where c is the velocity of sound in the fluid contained within the tube. For a non-dissipative medium, the infinitesimal pressure at the rigid end (where a = L) is given by

$$P = (\rho c A_0 \cos \omega t)/(\omega \sin kL). \tag{44}$$

If the medium is dissipative, the sound pressure at the rigid end is still given by Eq. 44, but now k may be considered as complex in order to account for the dissipation. We can now write Eq. 44 as

$$P = (\rho c_0 A_0/\omega)[\sinh^2 \alpha L + \sin^2 kL]^{-\frac{1}{2}} \cos \omega t \tag{45}$$

which is the same as Eq. 28 with a 90° phase change in the acceleration. And if the absorption is small (i.e., $\alpha L \ll 1$), the amplitude of Eq. 45 is given by Eq. 30

$$P \cong (\rho c_0 A_0/\omega)[(\alpha L)^2 + \sin^2 kL]^{-\frac{1}{2}} \tag{30}$$

This is of the form of a typical resonance curve if the width of the resonance curve is much less than the fundamental frequency. From this resonance curve, the half-power, or the "down 3dB" points, can be used to calculate the absorption in the resonance tube by

$$\alpha_{exp} = \pi/c\Delta f. \tag{46}$$

This method for determining the attenuation was used by Parker and by Henderson and Donnelley.

For the resonance tube, end effects seem to be the major additional consideration. If the losses at the ends are considered to be due only to heat conduction and are not a function of the viscosity, then an expression for these losses may be obtained by using the heat conduction portion of $\mathcal{V}'$.

The relationship of the viscous and heat conduction terms is given by Eq. 42

$$\gamma' = \sqrt{\sigma} + (\gamma - 1)(\sigma'/\sigma)^{1/2} \tag{42}$$

where the first term is the viscous term and the second term is the heat conduction term. Assume that the attenuations are additive, i.e., that

$$\alpha_{\gamma}(\text{total}) = \alpha_t + \alpha_e \tag{47}$$

where α_t is given by Eq. 41 and α_e is due to the losses at the end. Kirchhoff's expression for the attenuation due to the walls alone is

$$\alpha_w = (\sigma', c r_w)(\omega/2)^{1/2} \tag{48}$$

which becomes

$$\alpha_w = 2.976 \times 10^{-5} f^{1/2}/r_w \tag{49}$$

when evaluated for dry air at 23°C and atmospheric pressure. Equation 49 for tubes with a radius of 1.125 inches becomes

$$\alpha_w = 1.042 \times 10^{-3} f^{1/2} \quad (M^{-1}). \tag{50}$$

Assuming that the end has only heat conduction losses, then

$$\alpha_e \doteq 2[(\gamma-1)(\sigma'/\sigma)^{1/2}][(c r_w)^{-1}(\omega/2)^{1/2}][r_w^2/2L] \doteq (2\sigma'/3cr_w)(\omega/2)^{1/2}(r_w/2L) \tag{51}$$

Since the heat conduction term is approximately one-half the viscous term for dry air at 23°C and atmospheric pressure, the attenuation due to the ends can be related to the attenuation due to the walls by

$$\alpha_e \doteq \alpha_w \cdot r_w/3L \tag{52}$$

3.3.3 Experimental

Attenuation constants were experimentally measured for five identical resonance tubes of varying length by two methods. The first consisted of measuring the width of the infinitesimal-amplitude

resonance curve between the half-power points and using Eq. 46 to calculate the attenuation constant. This will be referred to as the Q method. The second method consisted of measuring the microphone and accelerometer output voltages at the resonant frequency and using Eq. 32 which can be written in terms of voltages

$$V_M = (\rho_o / \alpha_{exp} m \mathcal{V}) (S_M / S_A) V_A \qquad (53)$$

A plot of V_M vs V_A, for $\omega = \omega_p$, should result in a straight line of slope $(\rho_o / \alpha_{exp} m \mathcal{V})(S_M/S_A)$. From this slope, α_{exp} can be calculated if S_M and S_A are known. This method will be referred to as the A/P method.

3.3.4. Comparison of results

Attenuation constants were calculated for all five tubes using Eq. 49 and Shield's corrections for dry air at 23°C and 760 mmHg. These values for α_{cal} are compared with the experimentally determined α's for the fundamental modes in Table 1. The experimental results for all five tubes by both methods are compared with the theory in the range of interest in Figs. 3 and 4 where the log of the attenuation is plotted vs the log of the frequency. There is almost perfect agreement between the calculated and the experimentally observed attenuation constants by the Q method. This is true through the 50th harmonic for the 9' tube and the 40th harmonic for the 6' tube. At these points side modes were calculated to be present and were observed by distortion in the Q-curves.

Except for the 7 in. tube, the effect of the end-loss correction α_e is too small to see on the graphs. As a check on the end-loss approximation, if $\alpha_T = \alpha_{cal} + \alpha_c$ and α_{exp} in Table 1 are compared, it is seen that the assumption that the end losses are due solely

to heat conduction is slightly low. If the same losses are assumed for the ends as for the side wall, then an R/L relationship would hold. Again compare α_T and α_{exp} in Table 1, and it can be seen that this correction is too large indicating that the end correction is somewhere between these two extremes. If an empirical relationship of R/2L is taken, then the agreement is better than 1% for all but the seven inch tube.

The results of these investigations indicated that the Kirchhoff equation (using Shield's corrections and properly corrected for end losses) can be used to determine the attenuation in standing wave tubes of high Q where the boundaries approach ideal boundaries and where the length of the tube is much greater than the radius (on the order of ten to one).

The results further indicate that both the Q method and the A/P method are valid methods for determining the attenuation. The Q method has the advantage of requiring very little data and data processing to obtain the attenuation when a highly accurate frequency source is available. However, the acceleration had to be closely controlled, or an attenuation constant greater than actually existed was found. This change in the impedance of the driver near resonance could account for some of the problems in the past. The A/P method is reliable and useful when the frequency is not critical though the accelerometer and microphone must be accurately calibrated.

The effects of temperature cannot be minimized. A $3^{o}C$ change makes approximately a 1% change in Kirchhoff's constant for dry air as given by Eq. 42 and a resulting change in α . Also of interest is that a $0.6^{o}C$ temperature change will result in a 0.1 Hz change in ω_1 for the six foot tube. Therefore, it was important that the

temperature of the system be closely monitored, particularly when the resonance tube was being excited at very high levels.

3.4. Determination of the Resonance Frequency

The resonance frequency was determined by finding the frequency at which P_{11} was a maximum for a fixed A_o. Since ω_r was defined on the basis of the first-order solution, A_o was set low enough that finite-amplitude effects were negligible. Repeated measurements indicated that ω_r could be determined to better than 0.01 Hz providing consideration was given to temperature. As a check on ω_r, the frequencies of the "down 3 dB" points (which could be determined to within 0.001 Hz) were determined, and the mid-frequency was compared with ω_r. The agreement was within 0.005 Hz.

To arrive at a value of ω_r characteristic of the conditions actually prevailing at the time that the finite-amplitude data were collected, the experimental procedure was designed so that ω_r and the temperature were determined before the run and after the run and the temperature was recorded throughout the run. This technique insured that ω_r was known to within approximately 0.02 Hz for all runs.

3.5 System Alignment

It was necessary that the piston be very carefully aligned before each run or distortion was introduced into the input waveform. The system was designed so that the resonance tube was fixed and the shaker was mounted on an vibrational insulated base plate that was provided with three dimensional adjustment.

The alignment procedure consisted essentially of adjusting the piston in the tube until it was free to move. The piston was then excited at a low level, and the accelerometer output was monitored on

one trace of a dual trace oscilloscope. A sine wave from the frequency synthesizer was displayed on the other trace. Fine adjustment was made to the shaker base until the two wave forms appeared to be identical. The excitation level was then increased to the maximum level desired and additional fine adjustment was made as necessary.

The distortion present was determined by measuring with a wave analyzer the percentage of harmonic content relative to the fundamental in the accelerometer output. Due to the impedance mismatch between the accelerometer and the wave analyzer, it was necessary to use some form of impedance matching, and a Burr-Brown Model 100 preamplifier was used because it had a low noise and provided excellent isolation characteristics.

By using the visual method of waveform comparison for alignment, it was found that the second harmonic distortion of the acceleration waveform could be kept below 0.2% of the fundamental and the third harmonic distortion could be kept below 0.3% of the fundamental. All other harmonics were masked by the noise level.

4. Measurements and Analysis

Three measurement procedures were employed to compare the experimental results with the theory. These procedures provided information to compare the pressure waveforms, Q-curves, and a Fourier analysis of the waveforms with these quantities predicted by theory.

4.1. Pressure Waveform

The pressure waveforms for various sound pressure levels were compared with those predicted by the computer program FINAMPI. The program FINAMPI computes and graphs the predicted pressure waveform at the rigid end using all terms in the perturbation solution through the sixth order with input variables of ω, $\Delta\omega$, and M.

The measurement procedure consisted of first setting A_o and the frequency at either ω_m or at some desired frequency off resonance. The pressure waveform was then monitored on one channel of a dual-beam, dual-trace oscilloscope. A sine wave from the frequency synthesizer was displayed on the other channel for reference and distortion determination. Photographs were made of the oscilloscope trace for comparison purposes.

The analysis consisted simply of visually comparing the photographed pressure waveforms at the various SPL's and frequencies with those predicted by the computer program.

4.2. Fourier Analysis

A Fourier Analysis of the pressure waveform was made. The same procedure was used here as with the waveform analysis. In addition the harmonic content was measured as for the Q-curves.

The analysis consisted of applying a grid to the photograph and taking the amplitude of 64 equally spaced points in one cycle. These data points were used as the input for the computer program FOUANAL.FOUANAL takes these data points and does a Fourier snythesis on the wave shape. The amplitudes of the Fourier components were then compared with the measured values of the harmonics.

4.3. Q-Curves

It is possible to relate the response of the resonance tube to the frequency response of an electrical network. In this case the pressure curves of the resonance tube would be analogous to the "Q" response curves of the electrical network. Ruff has developed an expression for the amplitude of each harmonic of the pressure waveform as a function of $\Delta\omega$ and M. The procedures outlined here provided the means for displaying the harmonic content of the pressure wave as a function of frequency near resonance for a desired value of A_o.

The measurement procedure consisted of first setting the value of A_o and then measuring with a wave analyzer the pressure of the nth harmonic, P_{nn}, at the rigid end as a function of frequency. The frequency was swept from well below the half-power point to well above the half-power point for the fundamental in steps of 0.02 Hz. For the other harmonics through the sixth, the frequency was swept from just above the noise level through the area of interest back to just above the noise level in steps of 0.01 Hz.

The data were analyzed by first plotting the various P_{nn} in term of voltage versus the frequency. The data were then normalized using the magnitude of the leading term of the particular harmonic taken from the computer program QCURVE and QCURC. This was done to facilitate

comparison with the normalized graphs that were drawn by the computer. The fundamental resonance frequency was determined and used as the reference frequency for comparison with the computer graphs. The normalized data points for each harmonic were plotted and compared to the computer graphs provided by the two programs, QCURVE and QCURC.

QCURVES is a program that uses the perturbation solution and is designed to compute and graph the resonance response of each harmonic using terms of the sixth order as the fundamental is swept through resonance. QCURC is a program similar to QCURVES except that it uses the leading terms of each harmonic in the perturbation solution.

The major points considered were the amplitude of the harmonic, the frequency at which the maximum amplitude for each harmonic occurred, and the bandwidth of the various harmonics.

5. Results

In this section the experimental results will be compared with the theoretical results obtained by Ruff.

5.1. Pressure Waveforms

The first comparisons made will be of the pressure waveforms (Figs. 5-8). In these figures the large drawing is of the waveform predicted by the perturbation approach (program FINAMPI) and the smaller inset is a drawing from an oscilloscope photograph of the actual pressure waveform. The dashed line in both drawings is a sine wave which is included as a reference.

In the low Mach number region which includes Figs. 5 and 6, it appears that the theory and experiment are in very close agreement. In this region there is relatively little finite-amplitude distortion, and good agreement is expected. When the Mach number exceeds a value of about M = 0.005, the finite-amplitude distortion reaches a significant level. However, Fig. 7, which is for a Mach number of M = 0.007 indicates that the theoretical and experimental results are still in surprising agreement. As the Mach number is increased into the realm between significant finite-amplitude effects and the region of shock, the theory begins to breakdown as is evidenced in Fig. 8. This figure is for M = 0.009, and it is seen that the theoretical waveform displays details which are not observable in the experimental waveform.

It is evident that the theory becomes invalid when it is extended into the region of relatively high Mach number.

5.2. Fourier Analysis

In addition to the foregoing, the experimentally determined values of the amplitude of each harmonic may be compared with the results from the program FOUANAL.

The results of the comparison with the program FOUANAL are included in Table 2. FOUANAL uses the data taken point by point from an oscilloscope photograph and computes the Fourier coefficients of the various terms of a Fourier expansion of the waveform. The small size of the photographs and the thickness of the trace line in the photographs were such that only qualitative results were expected.

FOUANAL also computes the phase angle associated with each harmonic. These results are included in Table 3.

5.3. Q-Curves

Q-curves for three Mach numbers (M = 0.004, M = 0.005, M = 0.009) were experimentally obtained and graphed for comparison with the Q-curve program results for the same Mach numbers. These computer program results indicated by a dashed line for QCURVES and a solid line for QCURC are contained in Figs. 9 through 26. Several things should be mentioned concerning these graphs. First, the three Mach numbers chosen cover the range from very slight distortion to significant distortion and should indicate the usable extent of the theory. Second, in every figure, the Q-curve results from QCURVES, lies below the results obtained using QCURC (the first term method). The data points in general fall very close to the results of QCURC except for very high Mach numbers where the predicted amplitude of the higher harmonics is much larger than the experimentally determined. Another interesting fact is that the same harmonics for each Mach number have exactly the

same Q-curve using the first term method. This is not surprising when it is remembered that in the normalization scheme the dependence of the leading terms will not change for different Mach numbers.

5.4. General

It would have been interesting to obtain the same results for the other tubes used in the attenuation measurements, but time did not permit. However, some observations that were made are worthy of note. The distortion of the pressure waveform developed in the same way for all five tubes; however, in the formation of shock slight differences were noted and were more prominent in the short tube.

A sequence of photographs of the pressure waveforms for the 14 in., 6 ft., and 9 ft. tubes at sound pressure levels of 155, 157, and 160 dB were taken and are shown in Figs. 27, 28, and 29.

The wave shapes are very similar; however, there are certain noticable differences. The small spur at the base of the shock is present in all waveforms, but is more prominent in those for the 6 ft. tube. This point needs further investigation to determine whether the pressure actually decreases immediately before the shock or if the spur is due to some property of the instrumentation. The steepness of the shock front increases as the resonant frequency increases. The grass in the pressure waveform increases with an increase in resonant frequency and the drive level. This is a result of the "ringing" in the piston introduced by the shockwave banging against the piston face. The "grass" is also more prominently displayed at the higher frequencies due to the relative time scales and the higher drive levels required to attain the same sound pressure level. At very high drive levels, the

shock wave striking the piston can be observed in the accelerometer output from the piston, and its position can be shifted by small changes in the drive frequency.

6. Conclusions

Experimental investigation has shown that the theory accurately predicts the position relative to the fundamental at which the maximum amplitude of each harmonic occurs throughout the range from very low to very high Mach numbers. The investigation has also shown that in the region of relatively low Mach number the theory accurately predicts the amplitude of the first six harmonics that comprise the pressure waveform. The fact that the third harmonic is slightly high at the lower Mach numbers can be accounted for in part by the third harmonic distortion in the input. At high Mach numbers the predicted amplitudes of the higher harmonics are much greater than the experimentally observed ones. At this writing there is no definite explanation of this.

The reconstructed pressure waveforms drawn by the computer are in very close agreement with the experimentally observed ones at relatively low Mach numbers. When the finite-amplitude effects become pronounced, the theory does not properly predict the spur that forms just prior to the shock formation; however, the theory does indicate a definite distortion of the waveform in this region.

The Fourier analysis of the pressure waveform shows good agreement with the experimentally determined amplitudes at all Mach numbers. The experimental phase angles show an excessive scatter, and the agreement with the theoretical values is only qualitative. This appears to be the only place where the experimental results are less reliable than the theory. Since the major part of the distortion takes place in a relatively small portion of the waveform, the accuracy of the

Fourier analysis could be improved through the use of more data points in the region of the developing shock. It is suggested that further work along this line be postponed until the oscilloscope waveform can be more closely linked with the computer input.

In addition, the dependence of the theory on the infinitesimal-amplitude attenuation coefficient has been demonstrated.

In general, then the statement that the perturbation theory can adequately describe the effects of finite-amplitude standing waves in rigid-walled tubes has been shown to be valid provided the Mach number is such that the distortion is not too great. This of course corresponds to the pre-shock area, and even then precludes much of that area in which significant distortion is evident.

TUBE LENGTH	$\alpha_{cal} \cdot 10^2$ M^{-1}	$r/_{3L}$	$\alpha_e \cdot 10^2$ $(\alpha_{cal} \cdot r/_{3L}) \cdot 10^2$	$\alpha_t \cdot 10^2$ $(\alpha_{cal} + \alpha_e) \cdot 10^2$	$\alpha_{exp} \cdot 10^2$ M^{-1}	% DIFF
9'	0.832	0.0035	0.003	0.835	0.83	-0.6
6'	1.022	0.0051	0.005	1.027	1.03	0.3
28"	1.632	0.014	0.023	1.655	1.69	2.0
14"	2.307	0.027	0.063	2.370	2.45	3.2
7"	3.255	0.053	0.174	3.429	3.84	10.7

TUBE LENGTH	$\alpha_{cal} \cdot 10^2$ M^{-1}	$r/_{L}$	$\alpha_e \cdot 10^2$ $(\alpha_{cal} \cdot r/_{L}) \cdot 10^2$	$\alpha_t \cdot 10^2$ $(\alpha_{cal} + \alpha_e) \cdot 10^2$	$\alpha_{exp} \cdot 10^2$ M^{-1}	% DIFF
9'	0.832	0.0104	0.009	0.841	0.83	-1.2
6'	1.022	0.016	0.016	1.038	1.03	-0.8
28"	1.632	0.041	0.067	1.699	1.69	-0.5
14"	2.307	0.080	0.184	2.491	2.45	-1.6
7"	3.255	0.161	0.530	3.785	3.84	1.4

α_t = Attenuation constant using Weston's formula

α_{cal} = α_t + Shield's correction

α_e = Attenuation constant due to the end effect

= $\alpha_{cal} \cdot r/_{3L}$ or $\alpha_{cal} \cdot r/_{L}$

α_{exp} = Experimentally determined attenuation

ATTENUATION CONSTANTS AND END-EFFECT CALCULATIONS FOR FIVE RIGID-WALLED TUBES CONTAINING STANDING WAVES

TABLE 1

Method	Harmonic Number	Mach Number (M)			Method	Harmonic Number	Mach Number (M)		
		0.004	0.005	0.009			0.004	0.005	0.009
		Percent Harmonic					Percent Harmonic		
Experimental	2	11.8	17.0	21.1	Program QCURC	2	12.2	15.2	27.4
	3	3.3	5.8	9.6		3	3.5	5.4	17.5
	4	1.2	2.4	5.6		4	1.3	2.6	15.0
	5	0.52	1.1	3.8		5	0.6	1.4	14.7
	6	0.20	0.57	2.5		6	0.27	0.84	15.9
Program QCURVES	2	10.9	13.6	20.2	Program FOUANAL	2	12.0	17.5	23.1
	3	2.8	4.3	14.6		3	3.5	6.9	7.8
	4	1.1	1.8	8.6		4	1.7	3.3	4.1
	5	0.57	1.4	13.7		5	2.0	2.3	2.9
	6	0.27	0.82	13.9		6	0.93	1.03	2.0

Comparison of Experimental and Computer
Predicted Values of Harmonic Amplitude

Table 2

Program	Harmonic Number	Mach Number (M)		
		0.004	0.005	0.009
		Phase Angles (Radians)		
FOUANAL (Experimental)	1	0.0	0.0	0.0
	2	0.10	0.18	0.10
	3	0.58	0.54	0.45
	4	0.76	1.15	0.78
	5	0.93	1.71	1.15
	6	1.33	2.27	1.04
QUCURC	1		0.0	
	2		0.187	
	3		0.431	
	4		0.603	
	5		0.851	
	6		0.785	

Comparison of Experimental and Computer Predicted Values of Harmonic Phase Angles

Table 3

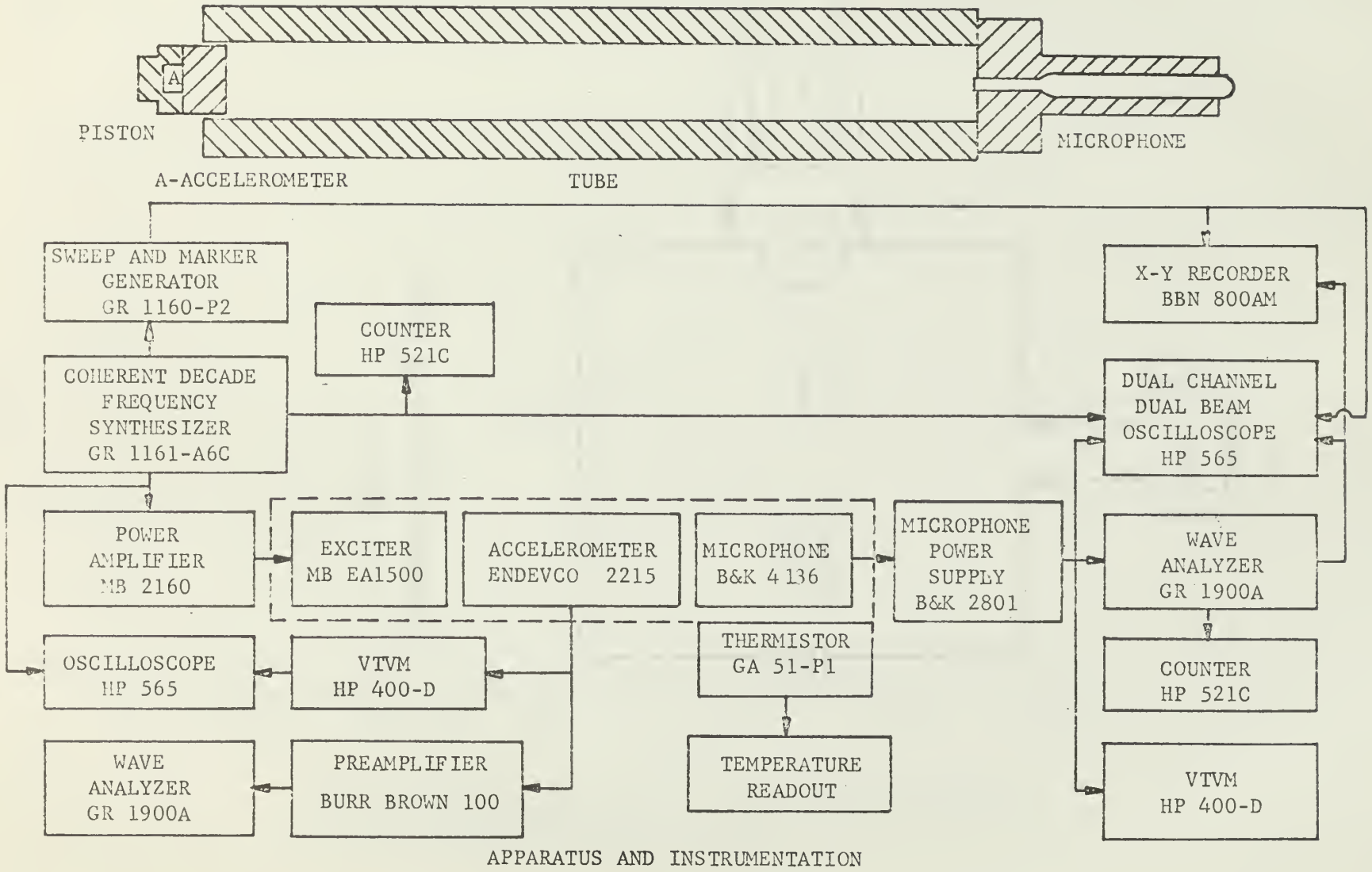
A
PISTON
MICROPHONE
A-ACCELEROMETER
TUBE
SWEEP AND MARKER GENERATOR GR 1160-P2
COUNTER HP 521C
COHERENT DECADE FREQUENCY SYNTHESIZER GR 1161-A6C
X-Y RECORDER BBN 800AM
DUAL CHANNEL DUAL BEAM OSCILLOSCOPE HP 565
POWER AMPLIFIER MB 2160
EXCITER MB EA1500
ACCELEROMETER ENDEVCO 2215
MICROPHONE B&K 4136
MICROPHONE POWER SUPPLY B&K 2801
WAVE ANALYZER GR 1900A
OSCILLOSCOPE HP 565
VTVM HP 400-D
THERMISTOR GA 51-P1
COUNTER HP 521C
WAVE ANALYZER GR 1900A
PREAMPLIFIER BURR BROWN 100
TEMPERATURE READOUT
VTVM HP 400-D
APPARATUS AND INSTRUMENTATION

FIGURE 1

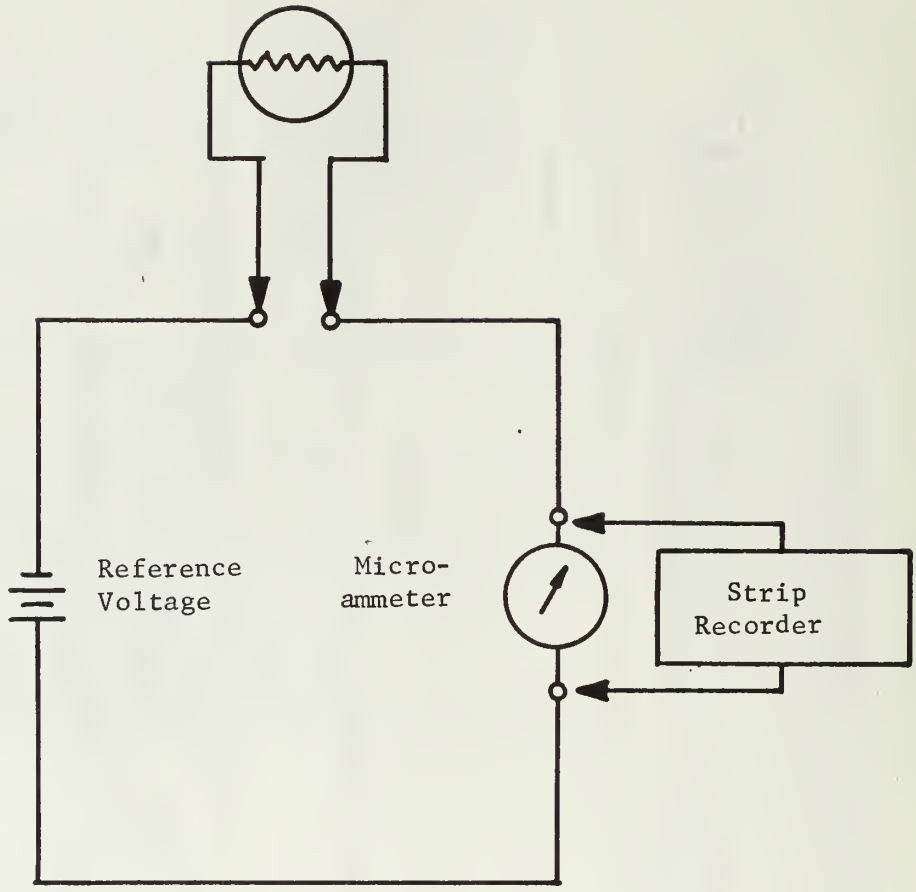

Temperature Monitoring System

Figure 2

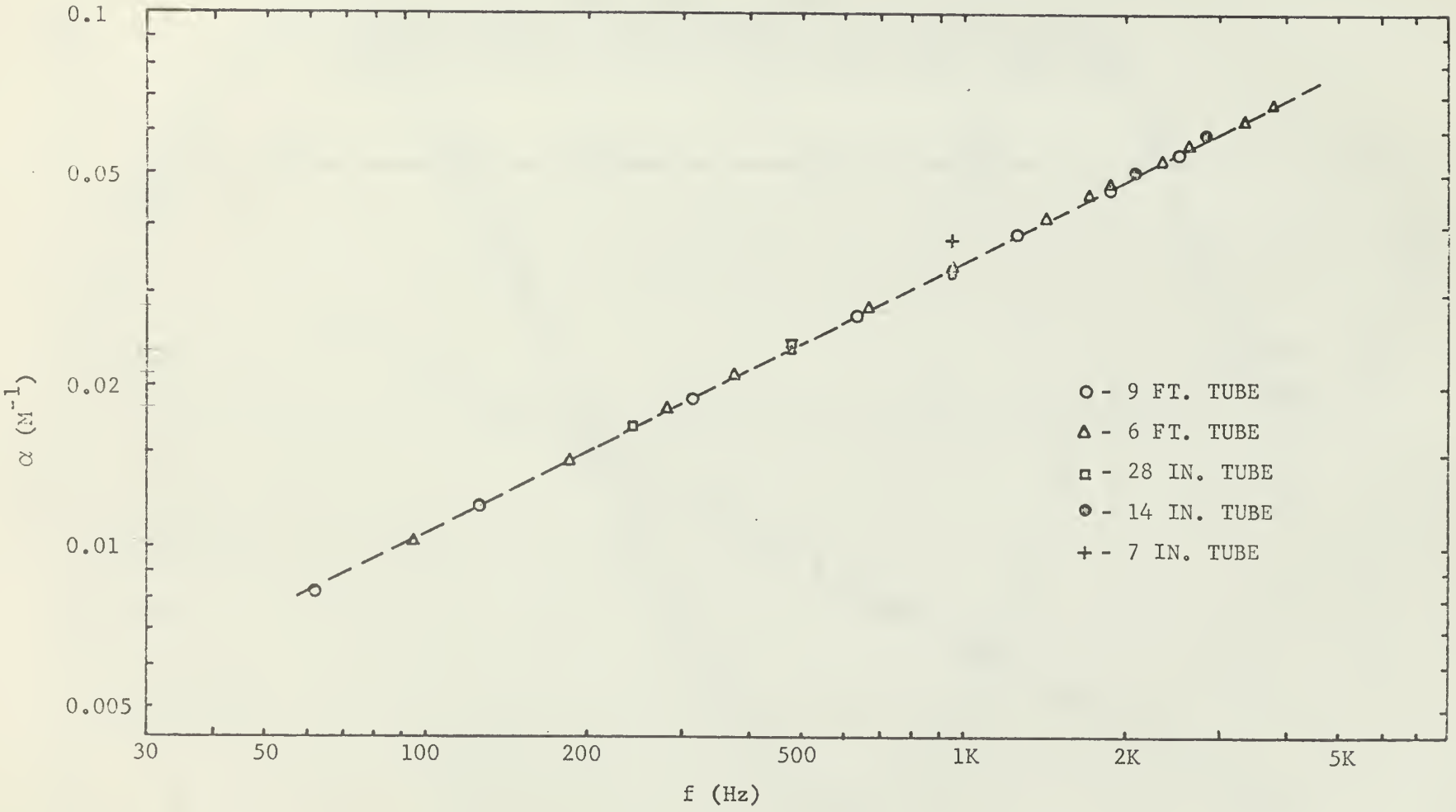

SOUND ABSORPTION IN AIR FOR RIGID-WALLED TUBES CONTAINING STANDING WAVES BY THE Q METHOD. — — — TUBE ABSORPTION, α_t, CALCULATED USING WESTON'S FORMULA

FIGURE 3

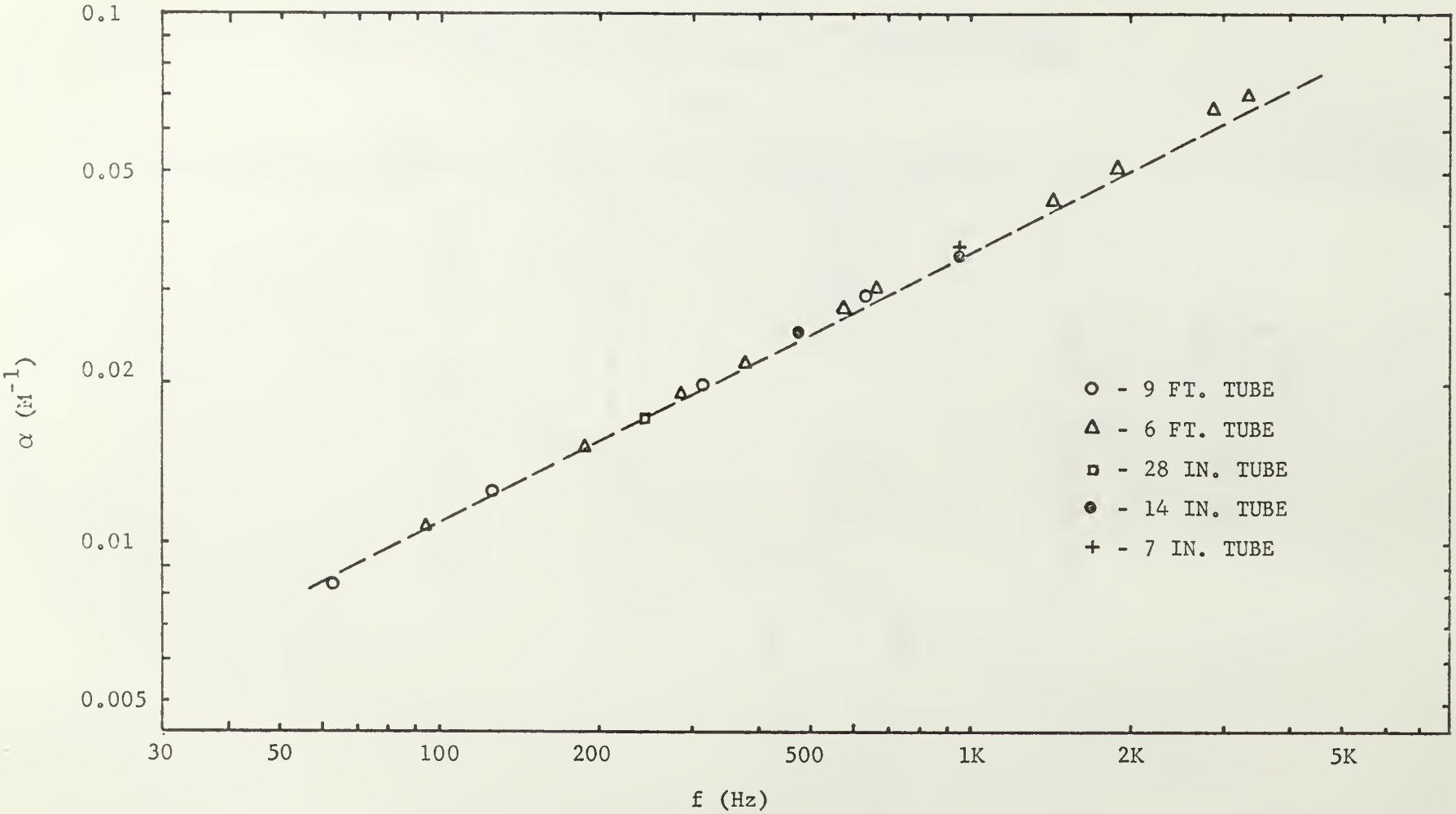

SOUND ABSORPTION IN AIR FOR RIGID-WALLED TUBES CONTAINING STANDING WAVES BY THE A/P METHOD. — — —TUBE ABSORPTION, α_t, CALCULATED USING WESTON'S FORMULA

FIGURE 4

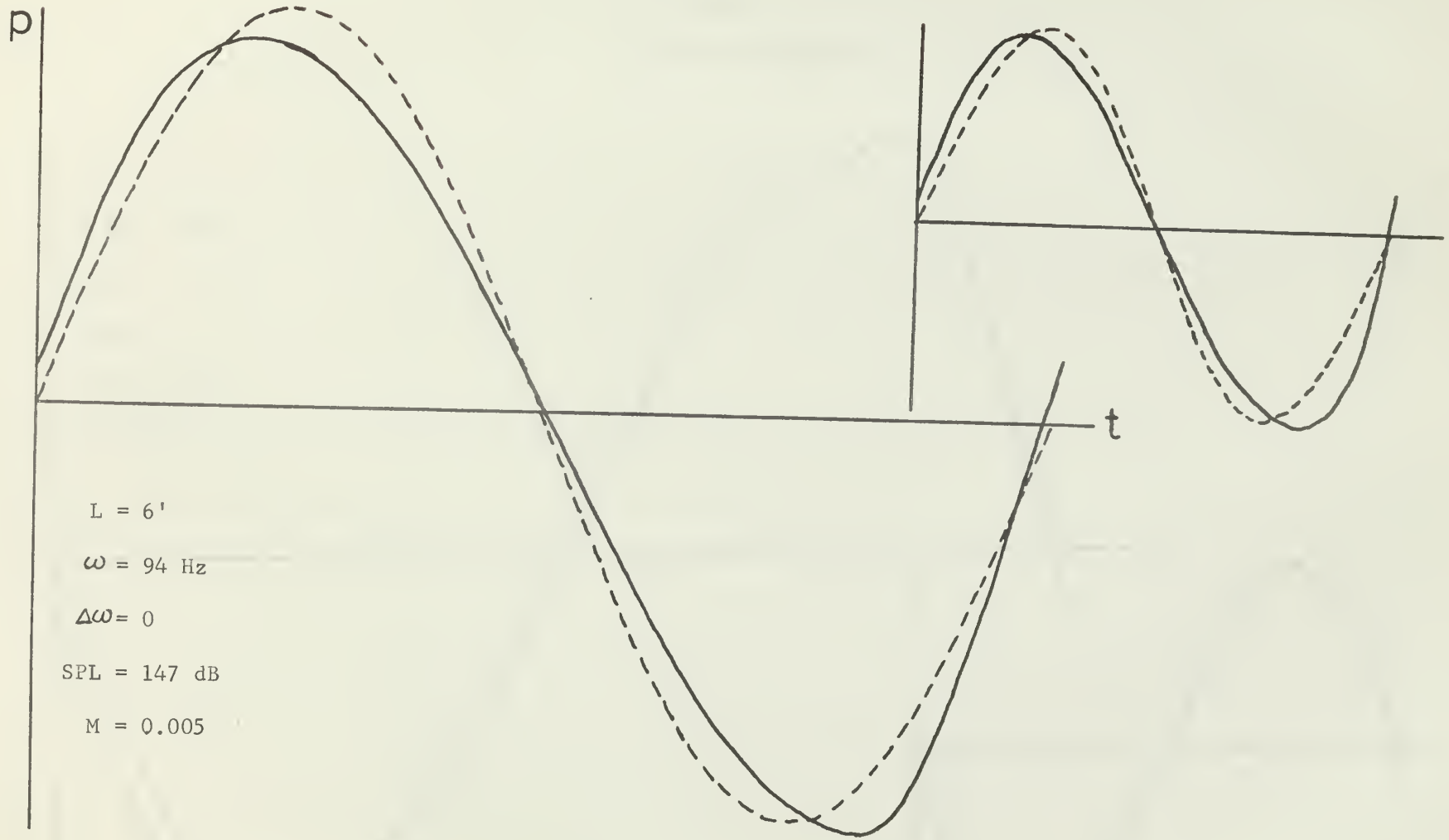

Pressure Waveforms

Figure 5

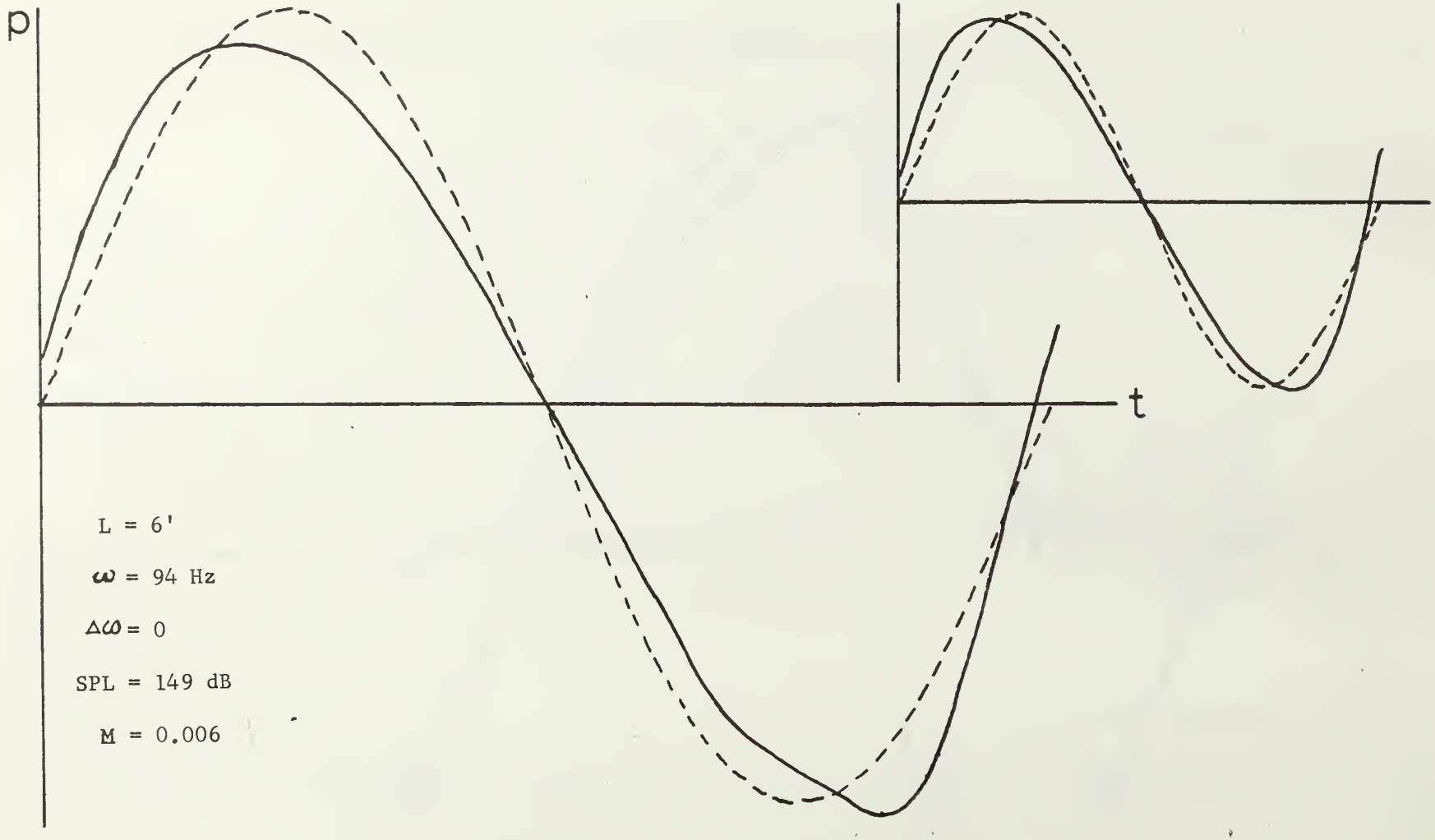

Pressure Waveforms

Figure 6

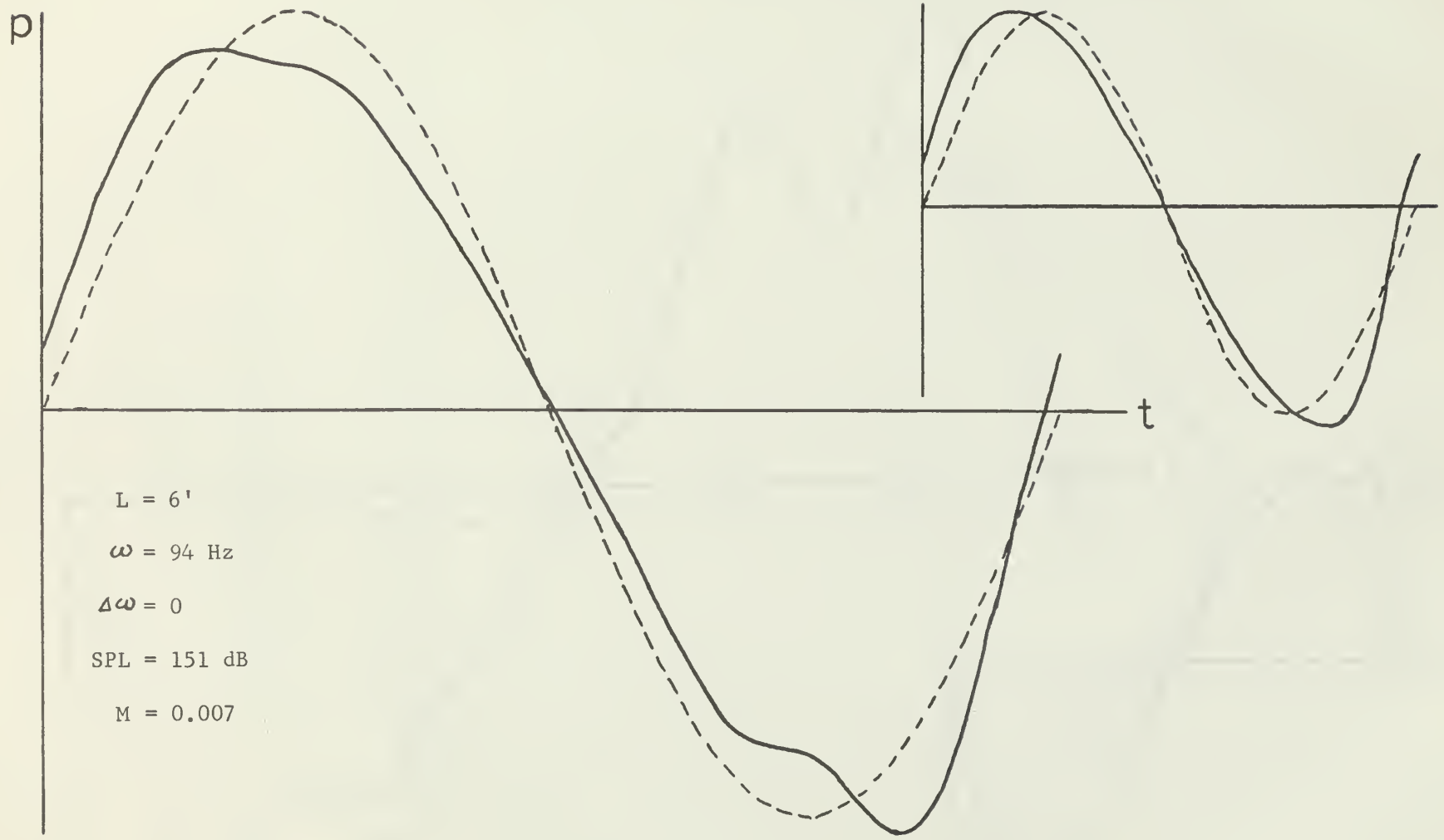

Pressure Waveforms

Figure 7

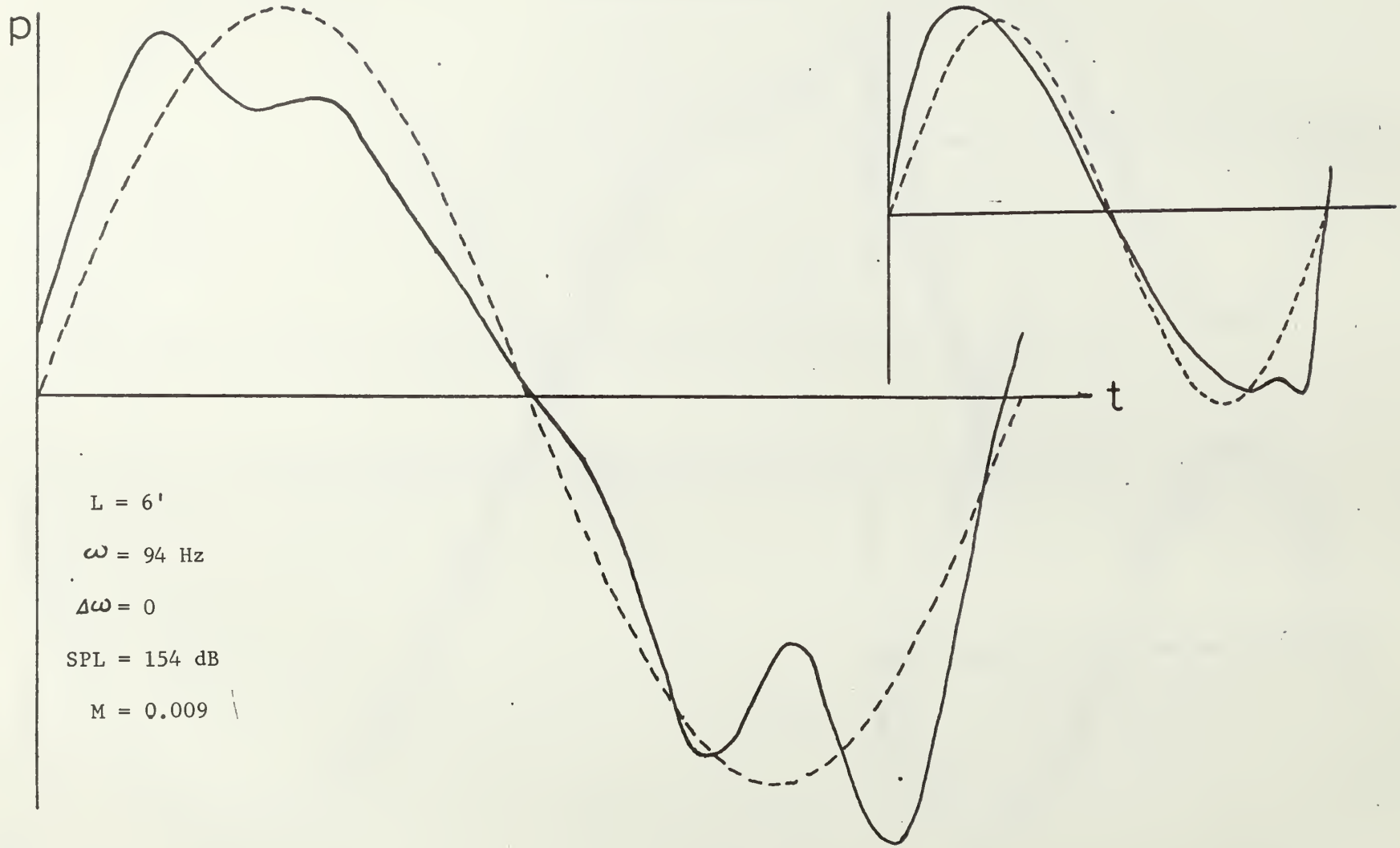

Figure 8

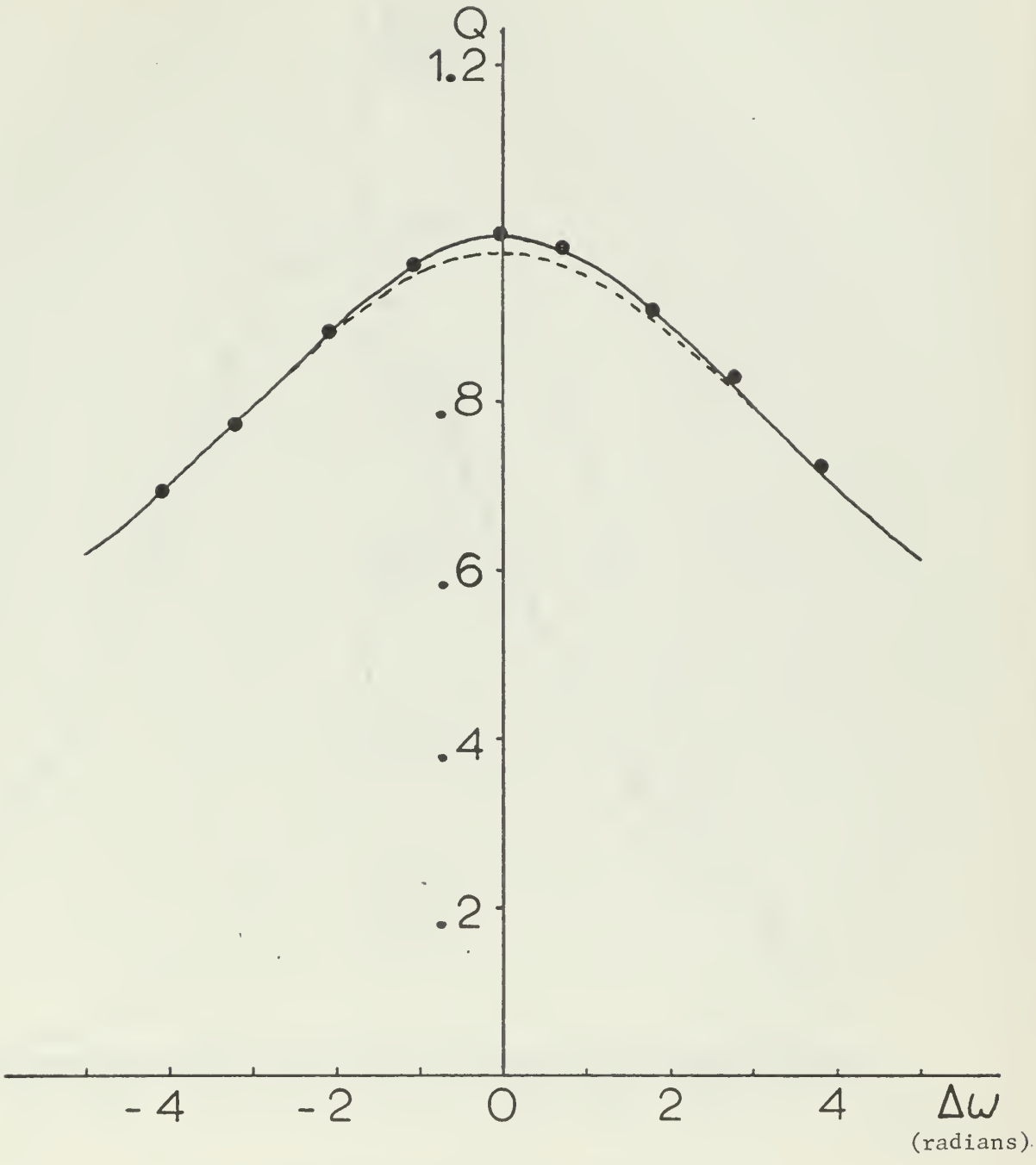

Q-curves of the Fundamental Harmonic
M = 0.004, SPL = 147 dB, L = 6'

Figure 9

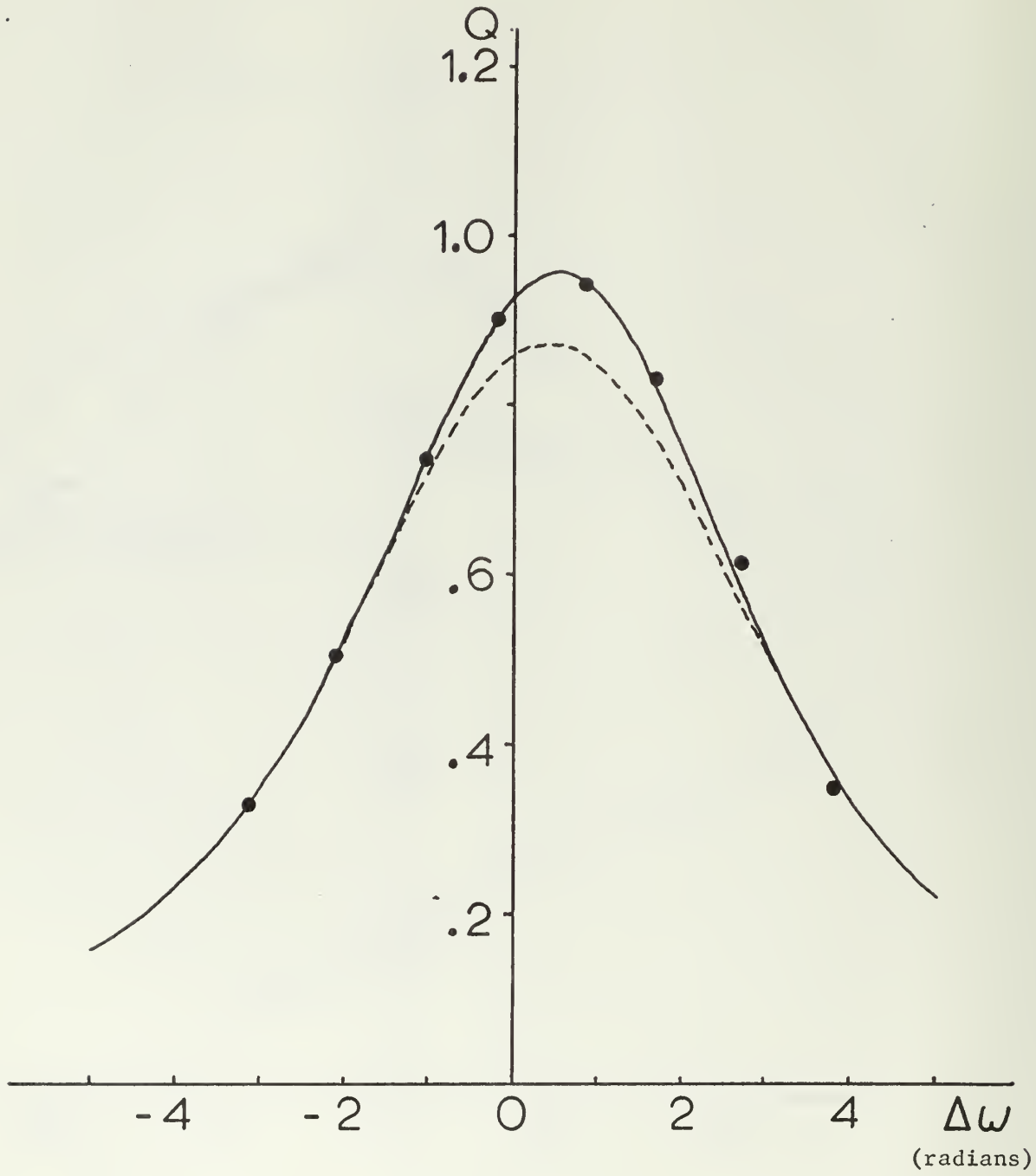

Q-curves of the Second Harmonic
M = 0.004, SPL = 147 dB, L = 6'

Figure 10

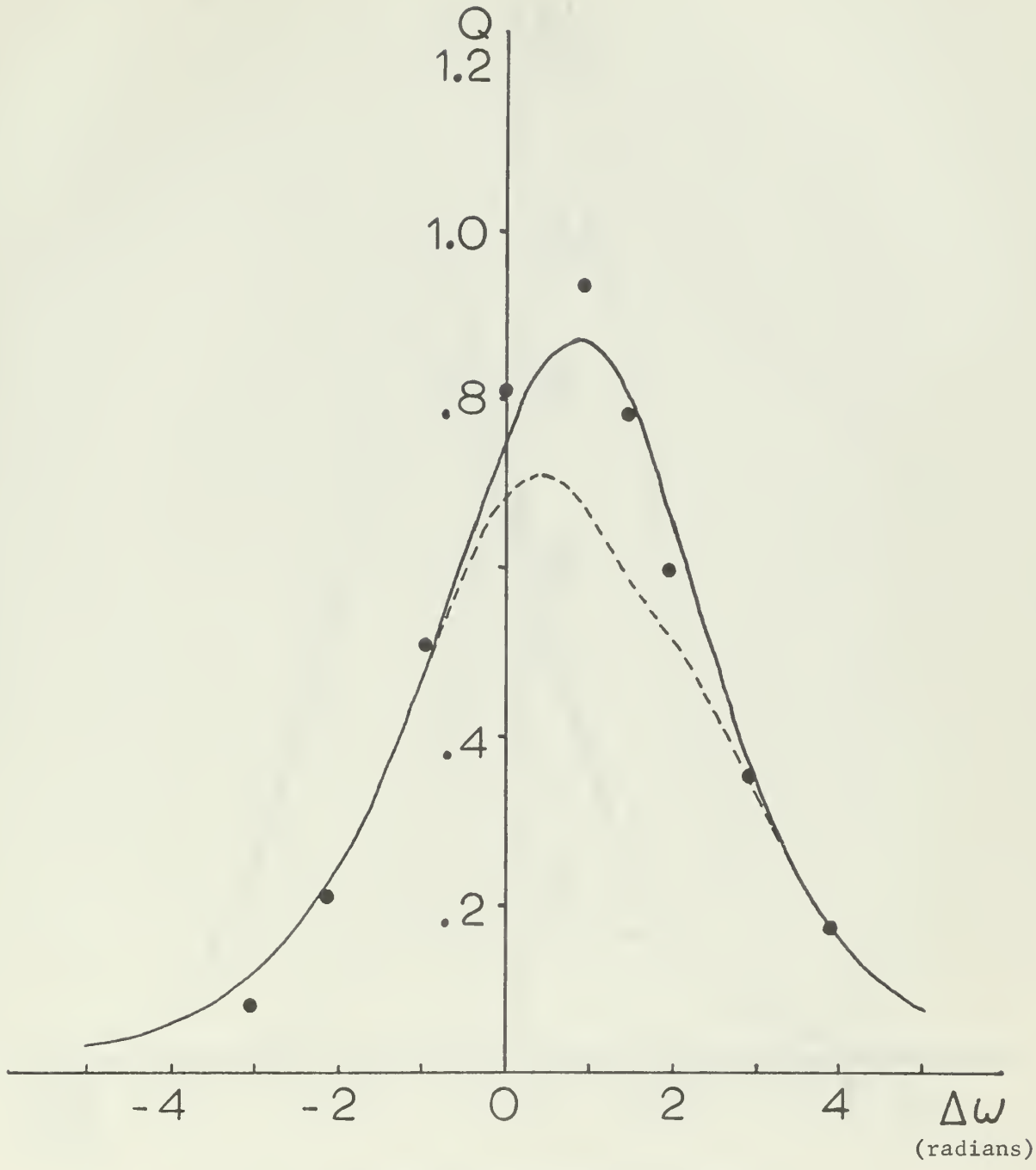

Q-curves of the Third Harmonic
M = 0.004, SPL = 147 dB, L = 6'

Figure 11

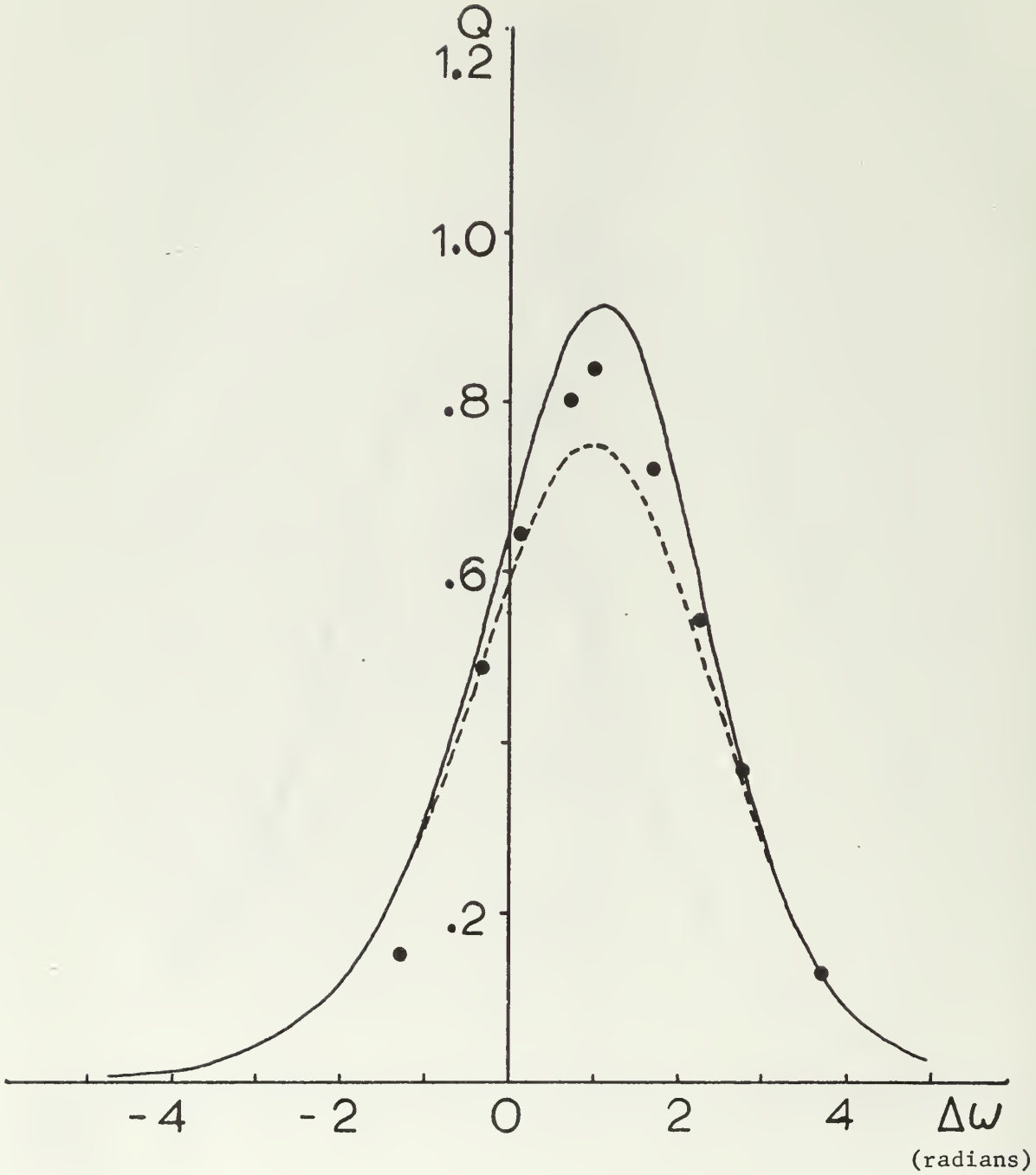

Q-curves of the Fourth Harmonic
M = 0.004, SPL = 147 dB, L = 6'

Figure 12

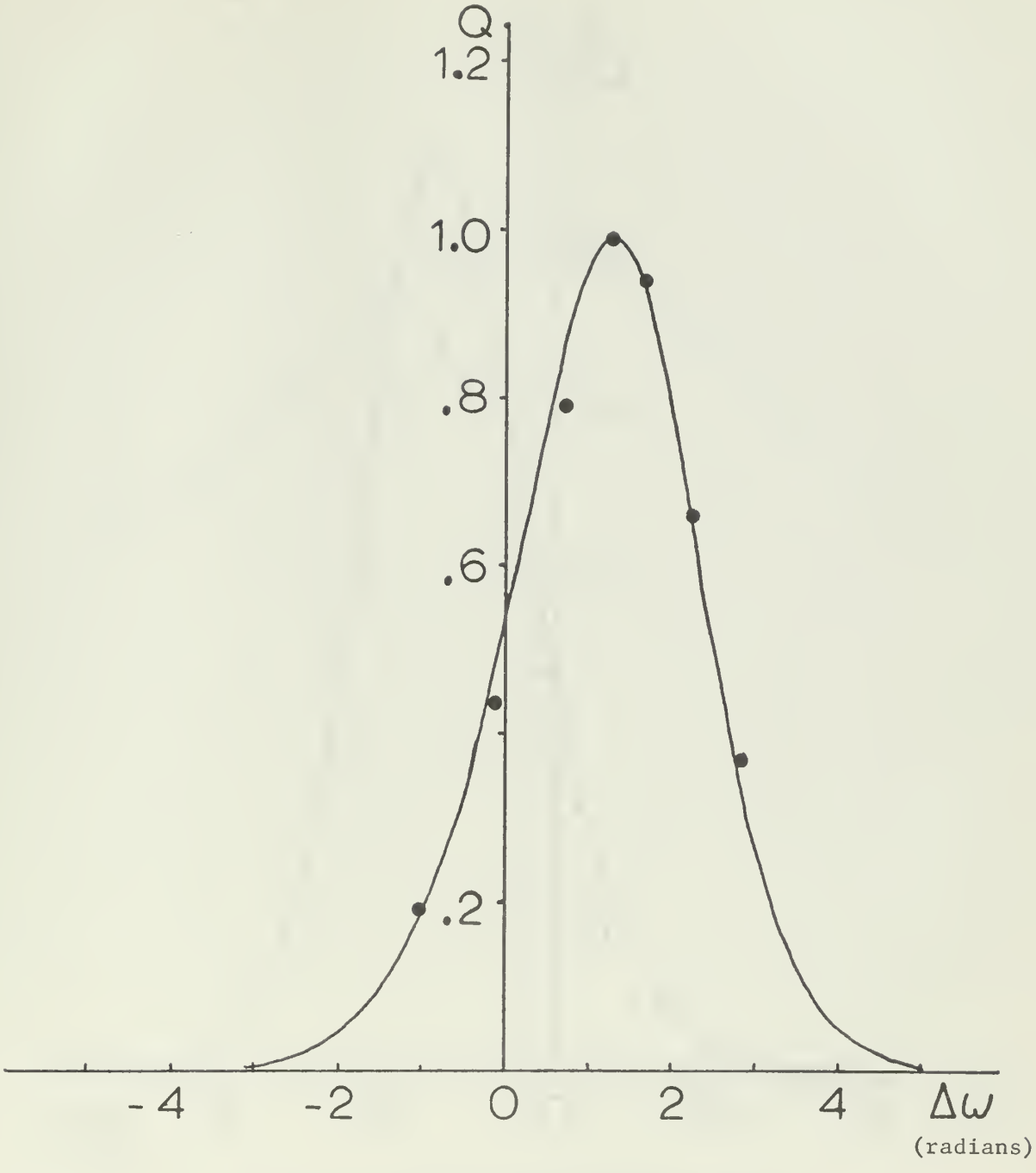

Q-curves of the Fifth Harmonic
M = 0.004, SPL = 147 dB, L = 6'

Figure 13

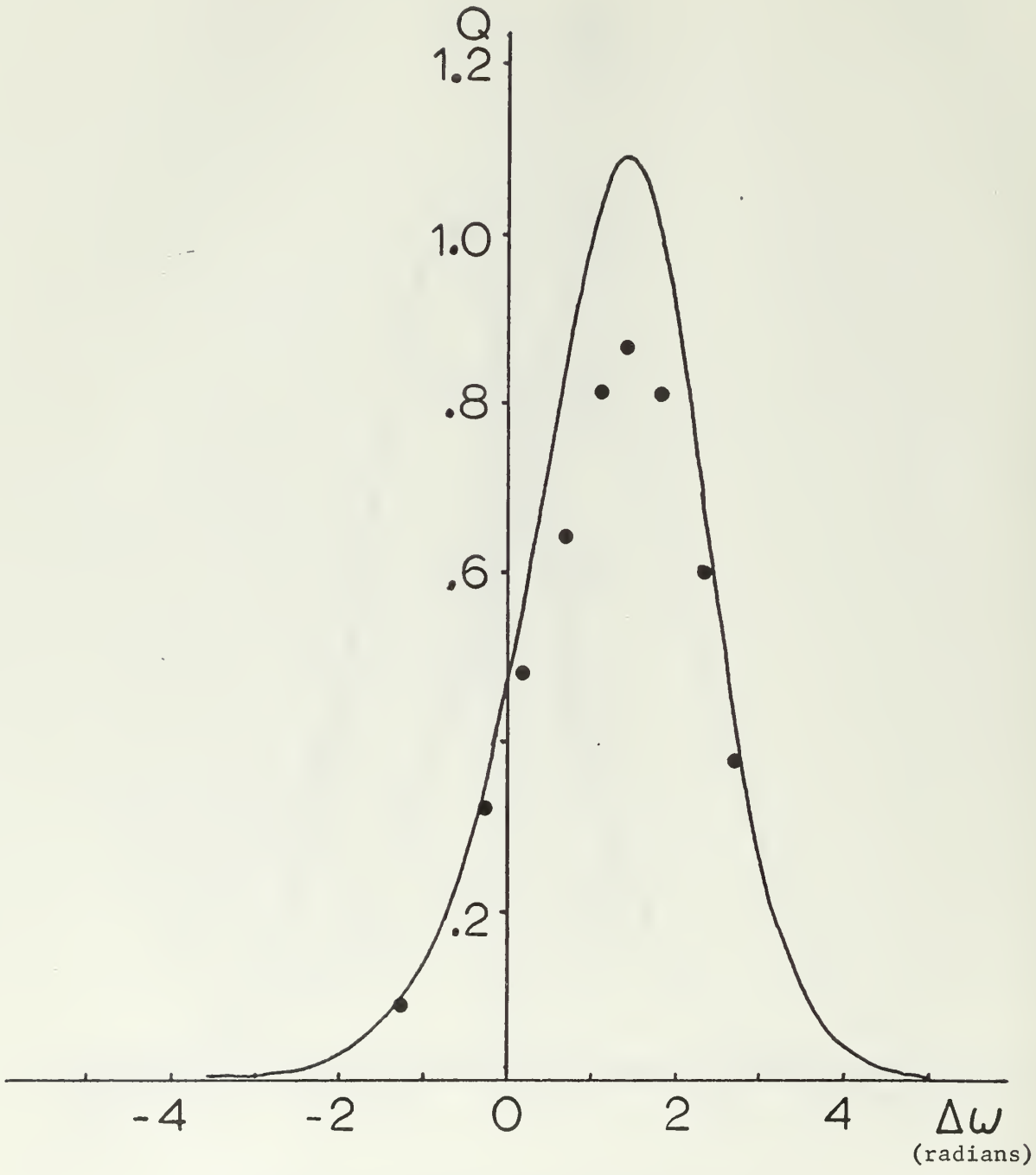

Q-curves of the Sixth Harmonic
M = 0.004, SPL = 147 dB, L = 6'

Figure 14

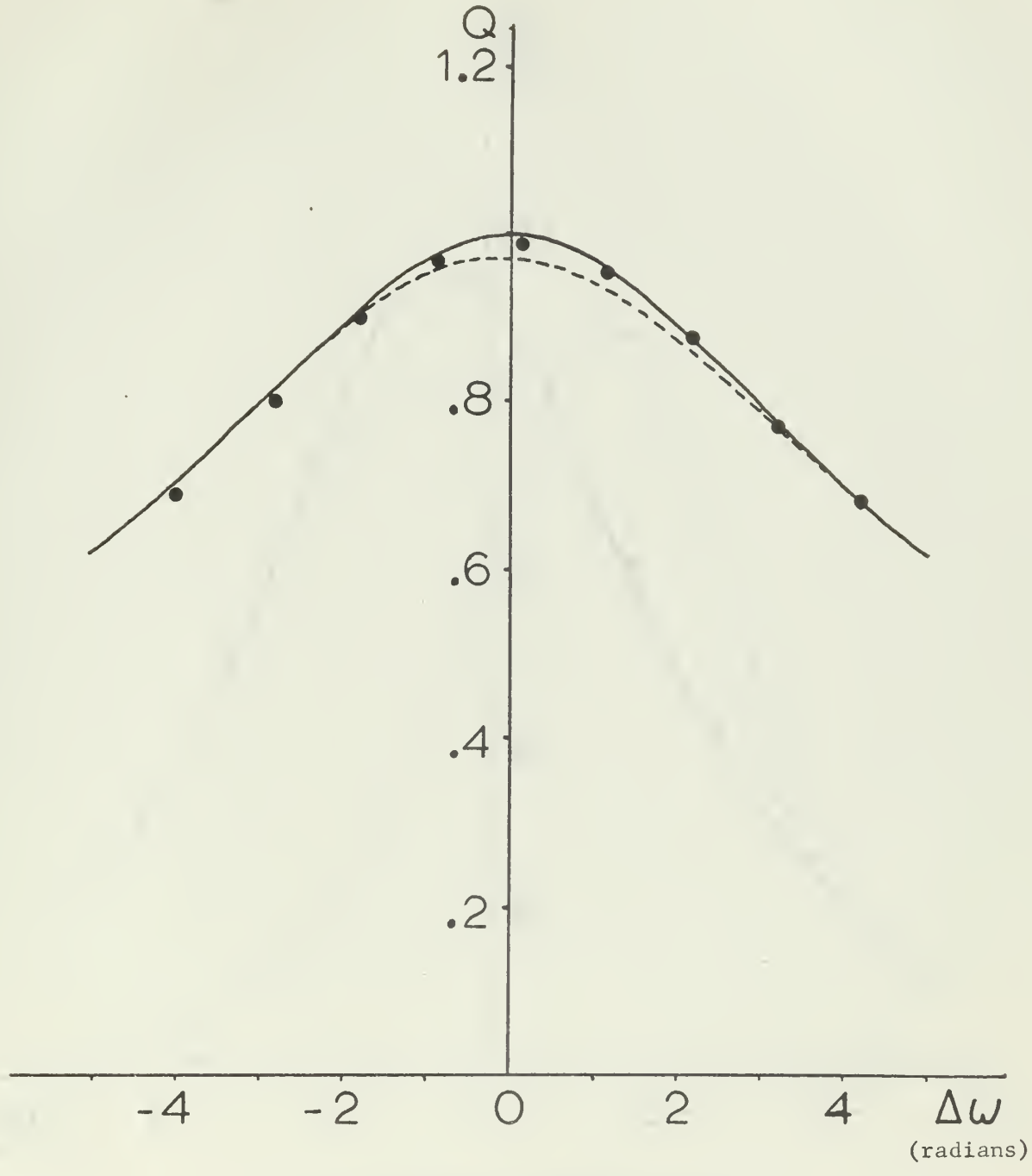

Q-curves of the Fundamental Harmonic,
M = 0.005, SPL = 149 dB, L = 6'

Figure 15

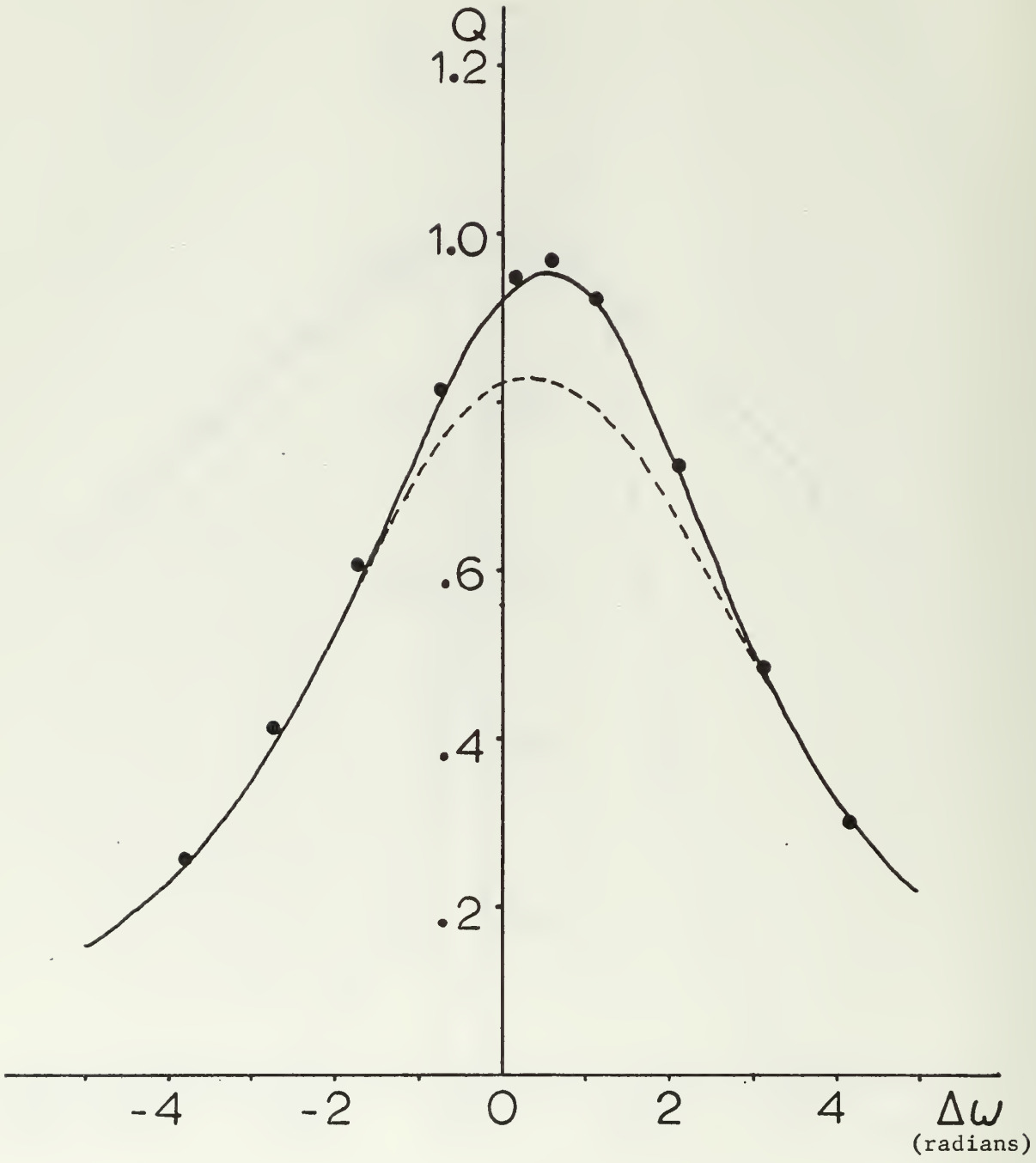

Q-curves of the Second Harmonic,
M = 0.005, SPL = 149 dB, L = 6'

Figure 16

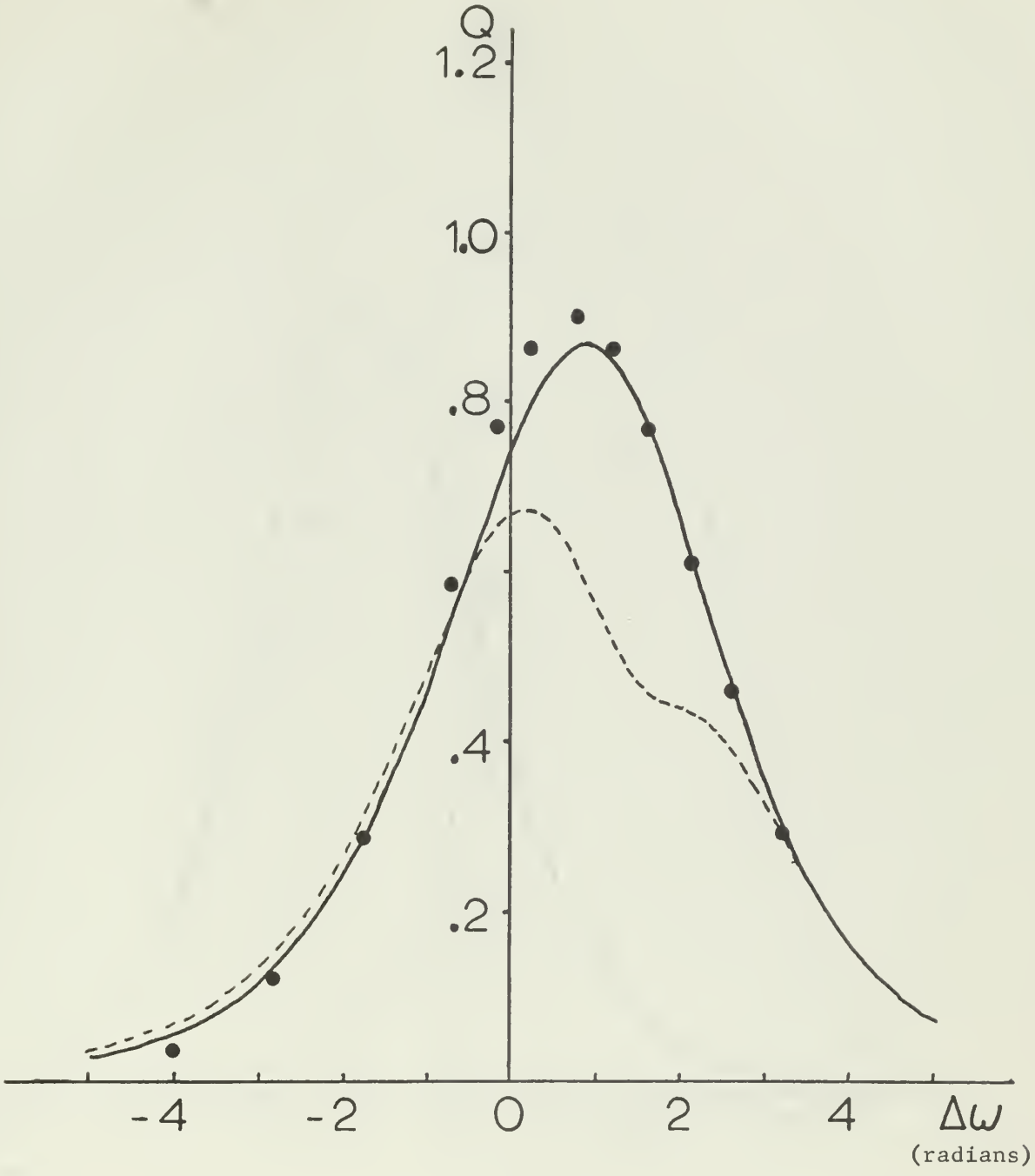

Q-curves of the Third Harmonic,
M = 0.005, SPL = 149 dB, L = 6'

Figure 17

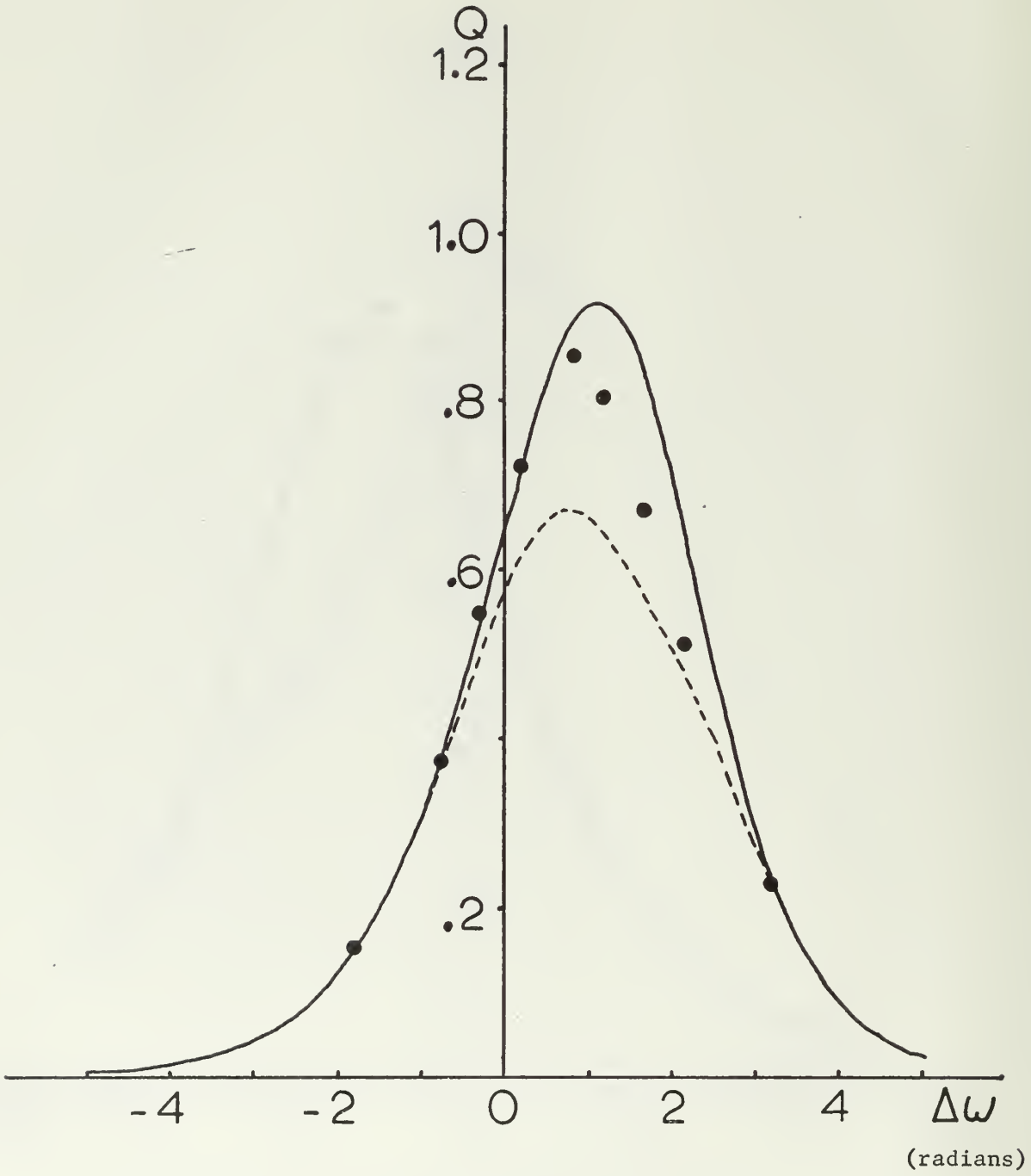

Q-curves of the Fourth Harmonic,
M = 0.005, SPL = 149 dB, L = 6'

Figure 18

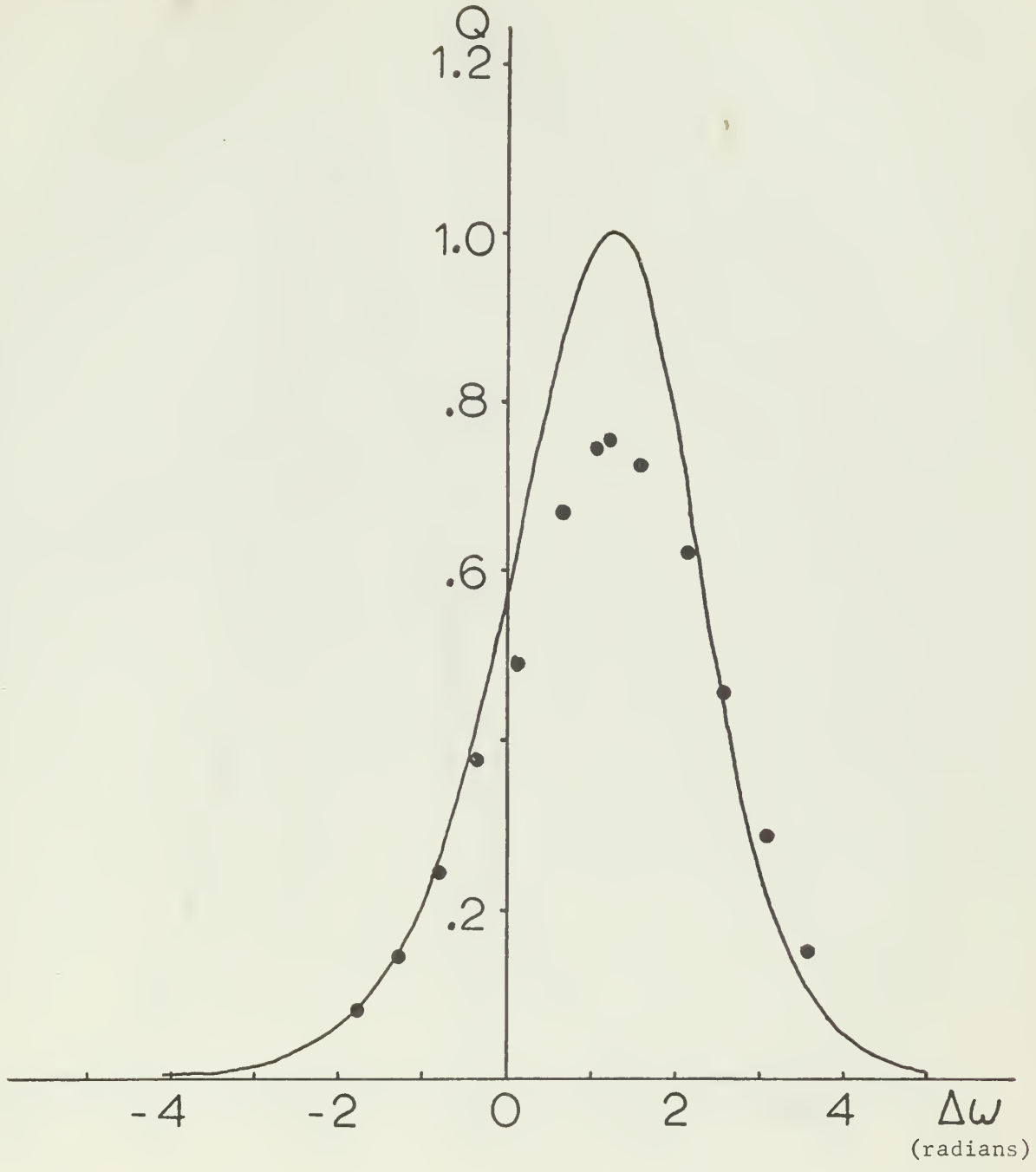

Q-curves of the Fifth Harmonic,
M = 0.005, SPL = 149 dB, L = 6'

Figure 19

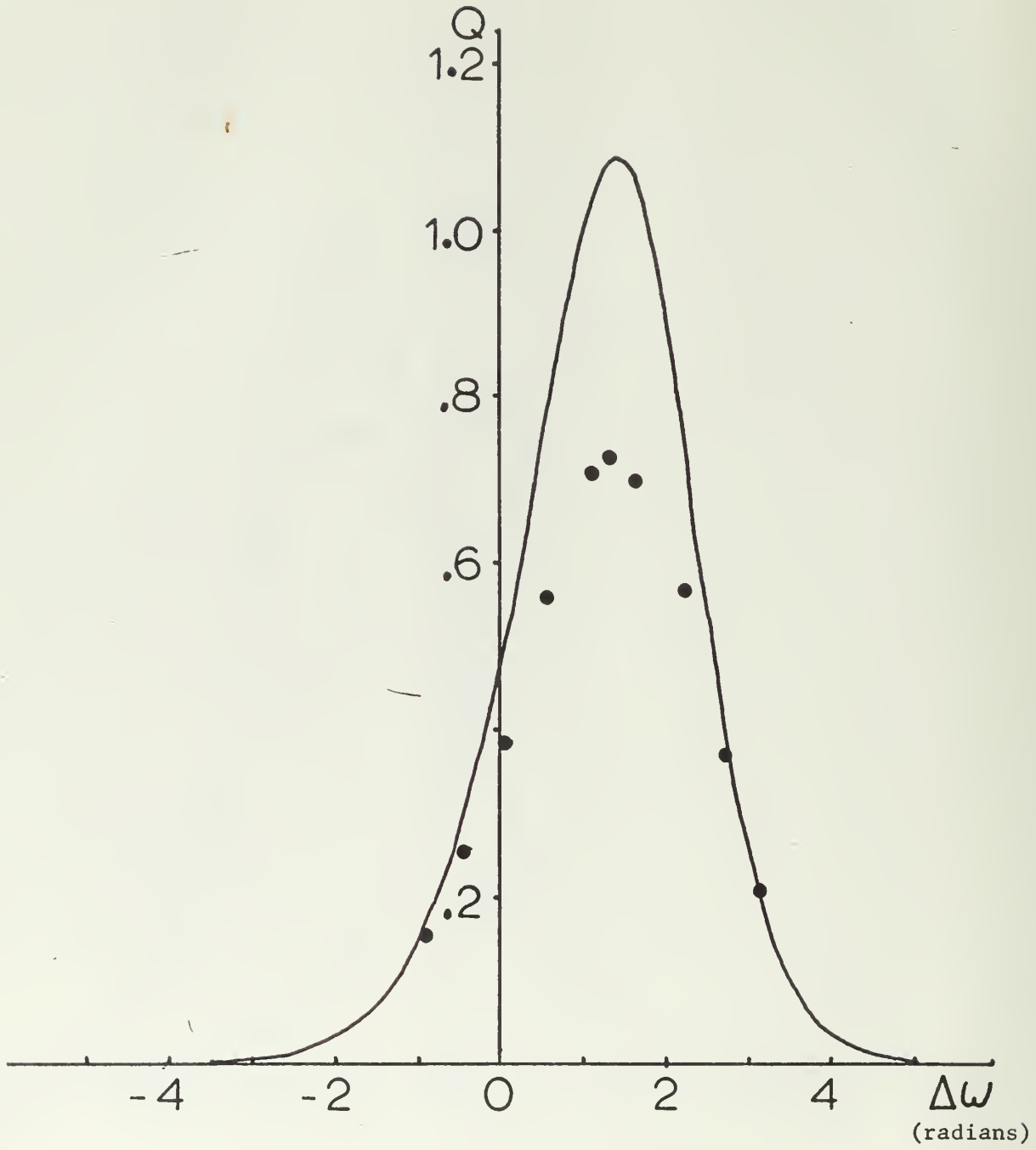

Q-curves of the Sixth Harmonic,
M = 0.005, SPL = 149 dB, L = 6'

Figure 20

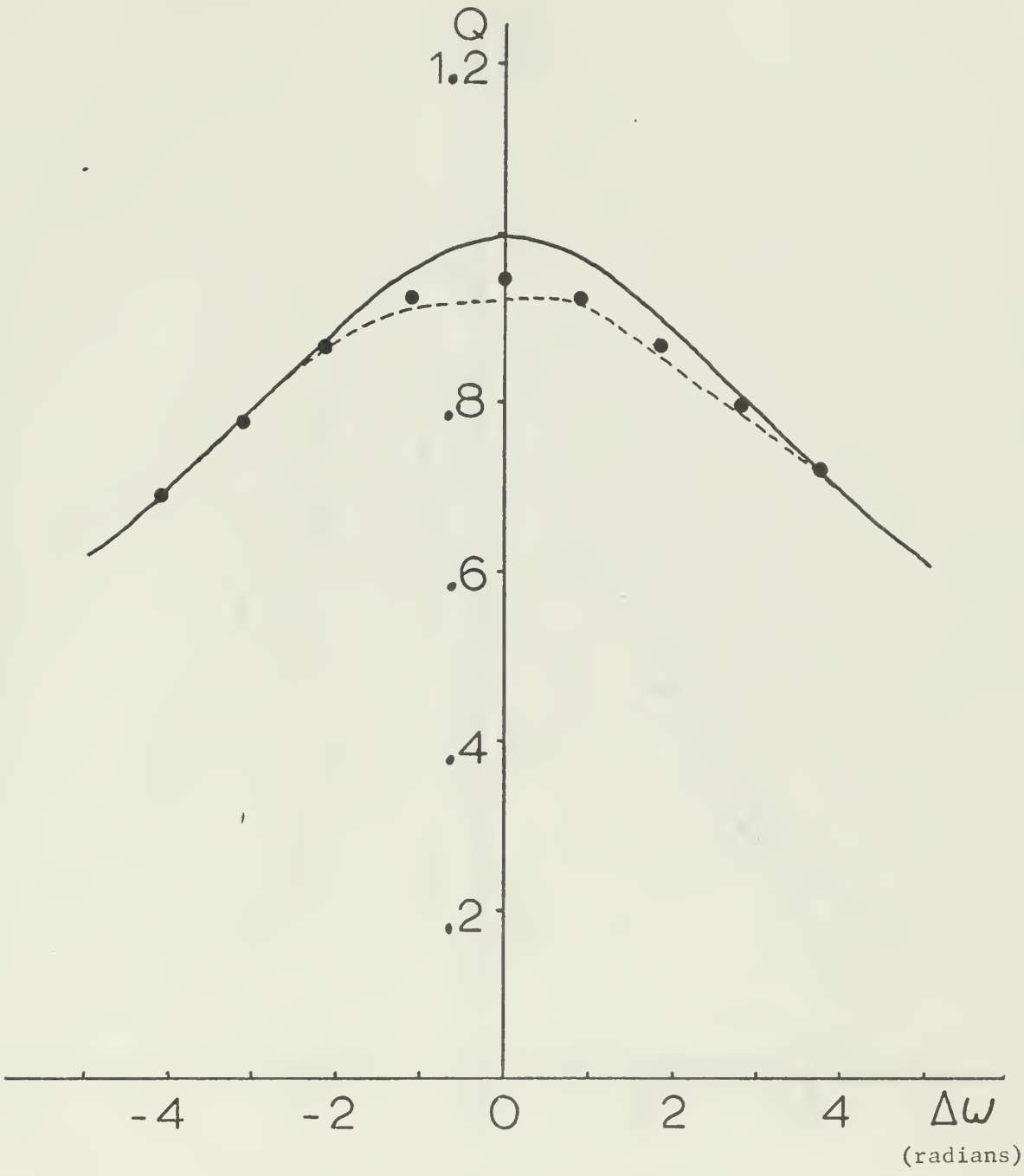

Q-curves of the Fundamental Harmonic,
M = 0.009, SPL = 154 dB, L = 6'

Figure 21

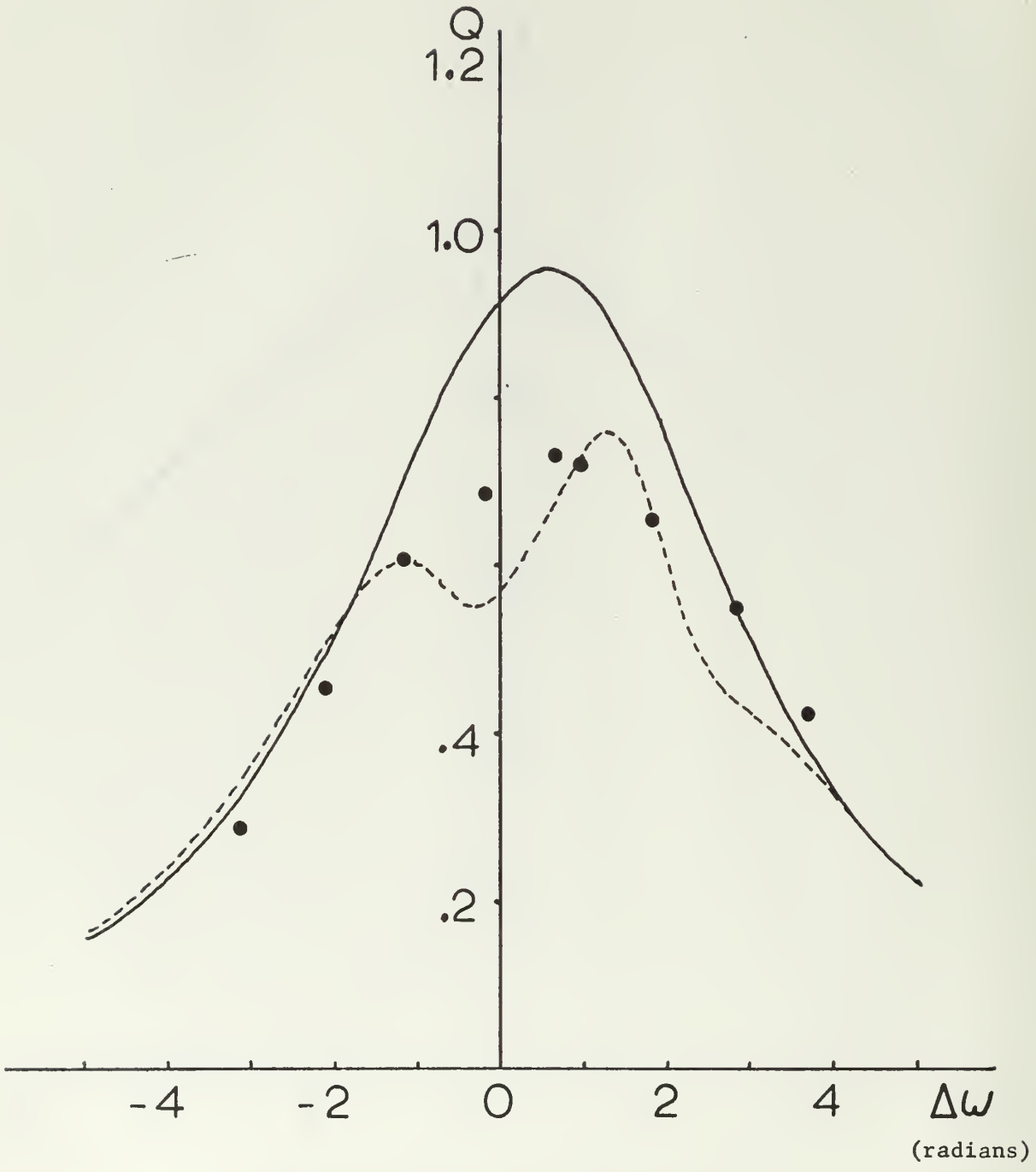

Q-curves of the Second Harmonic,
M = 0.009, SPL = 154 dB, L = 6'

Figure 22

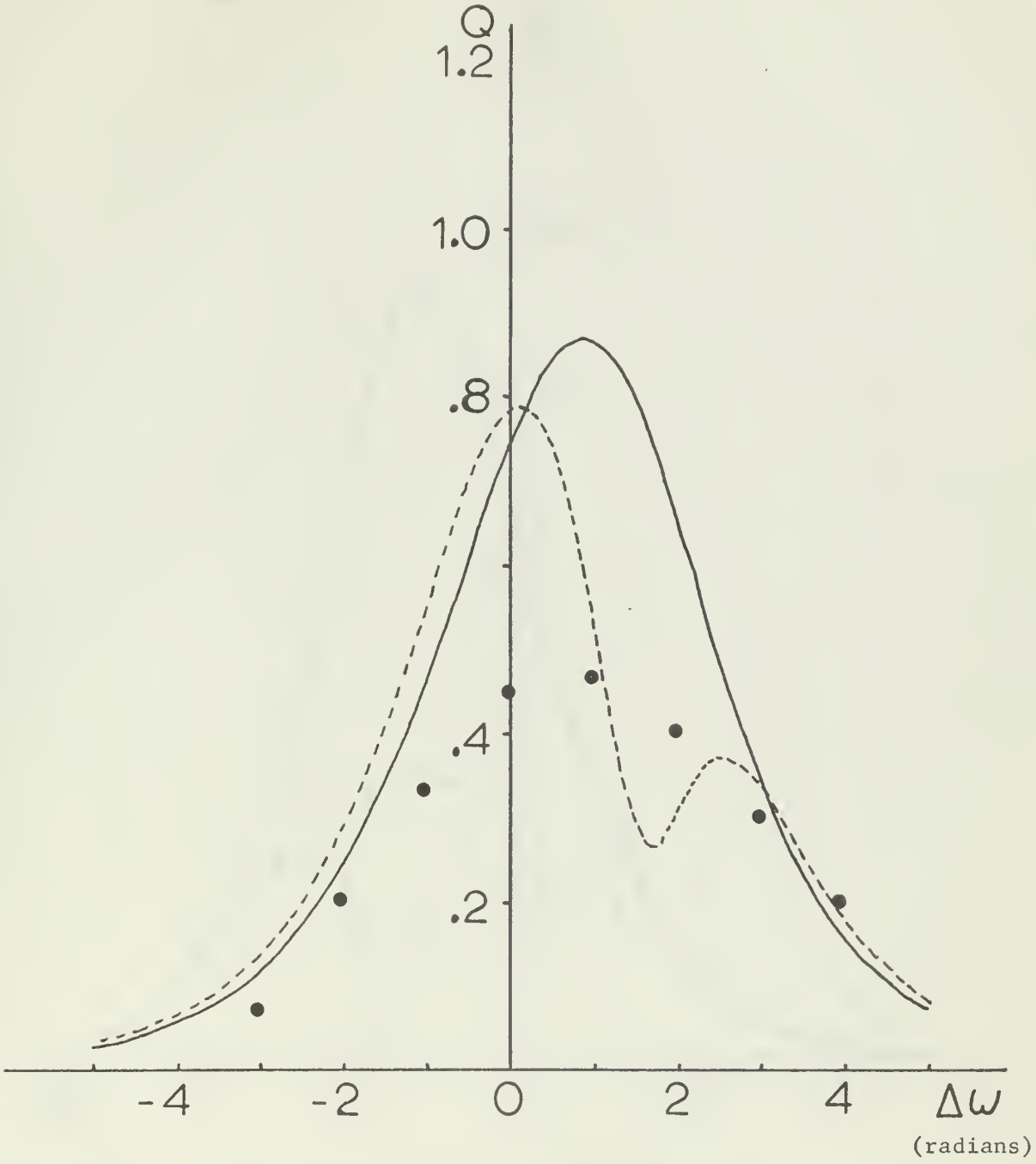

Q-curves of the Third Harmonic,
M = 0.009, SPL = 154 dB, L = 6'

Figure 23

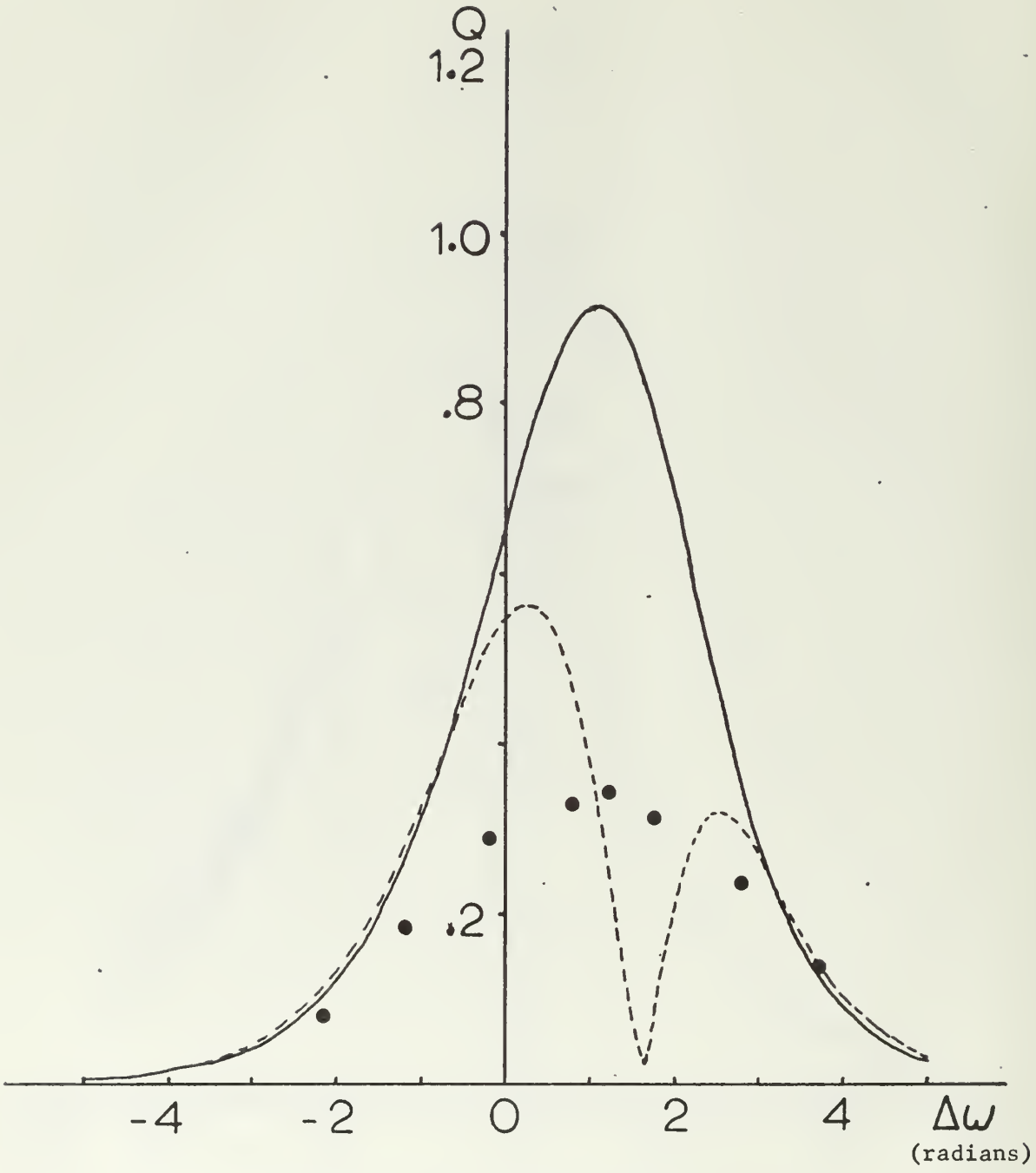

Q-curves of the Fourth Harmonic,
M = 0.009, SPL = 154 dB, L = 6'

Figure 24

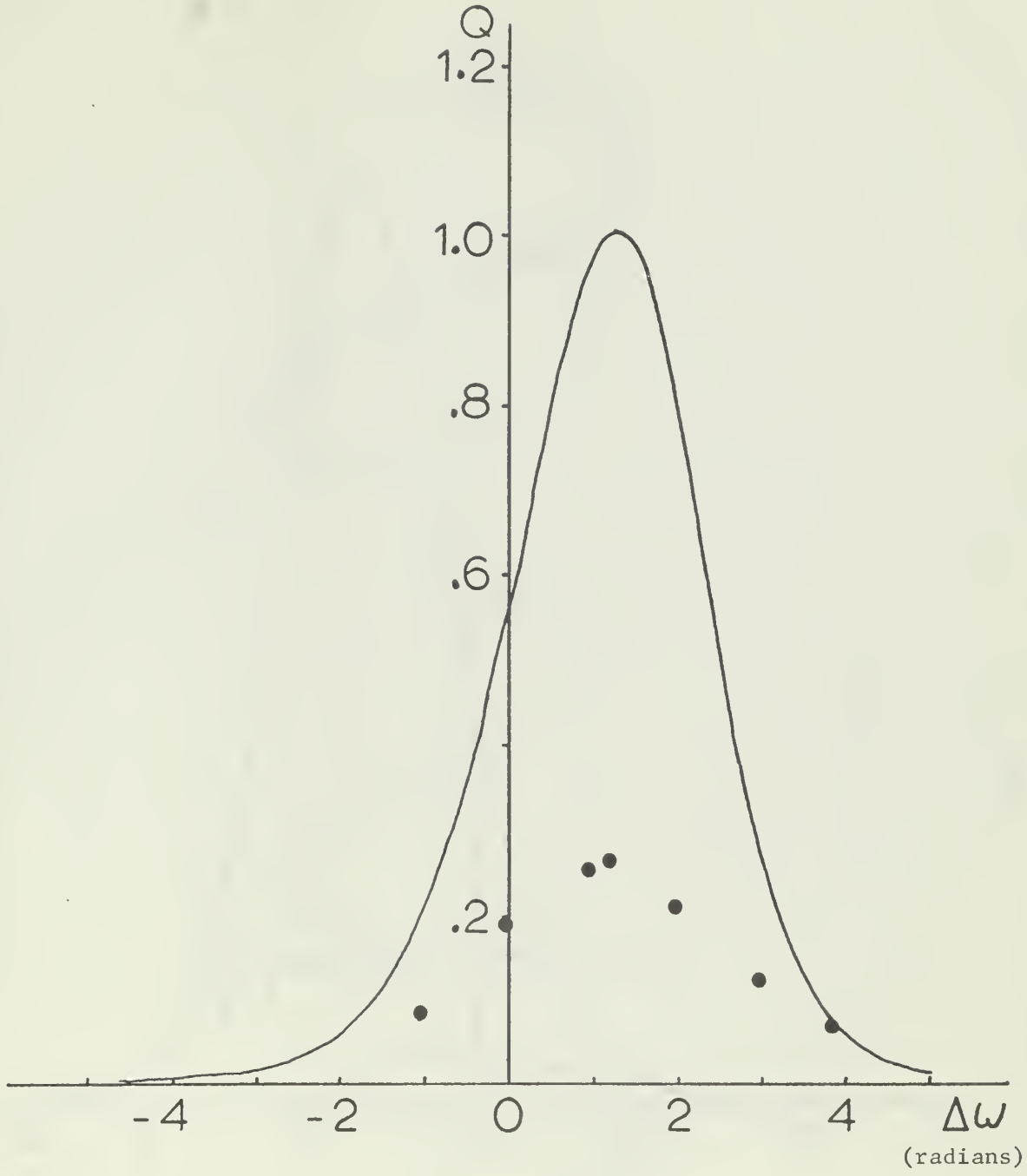

Q-curves of the Fifth Harmonic,
M = 0.009, SPL = 154 dB, L = 6'

Figure 25

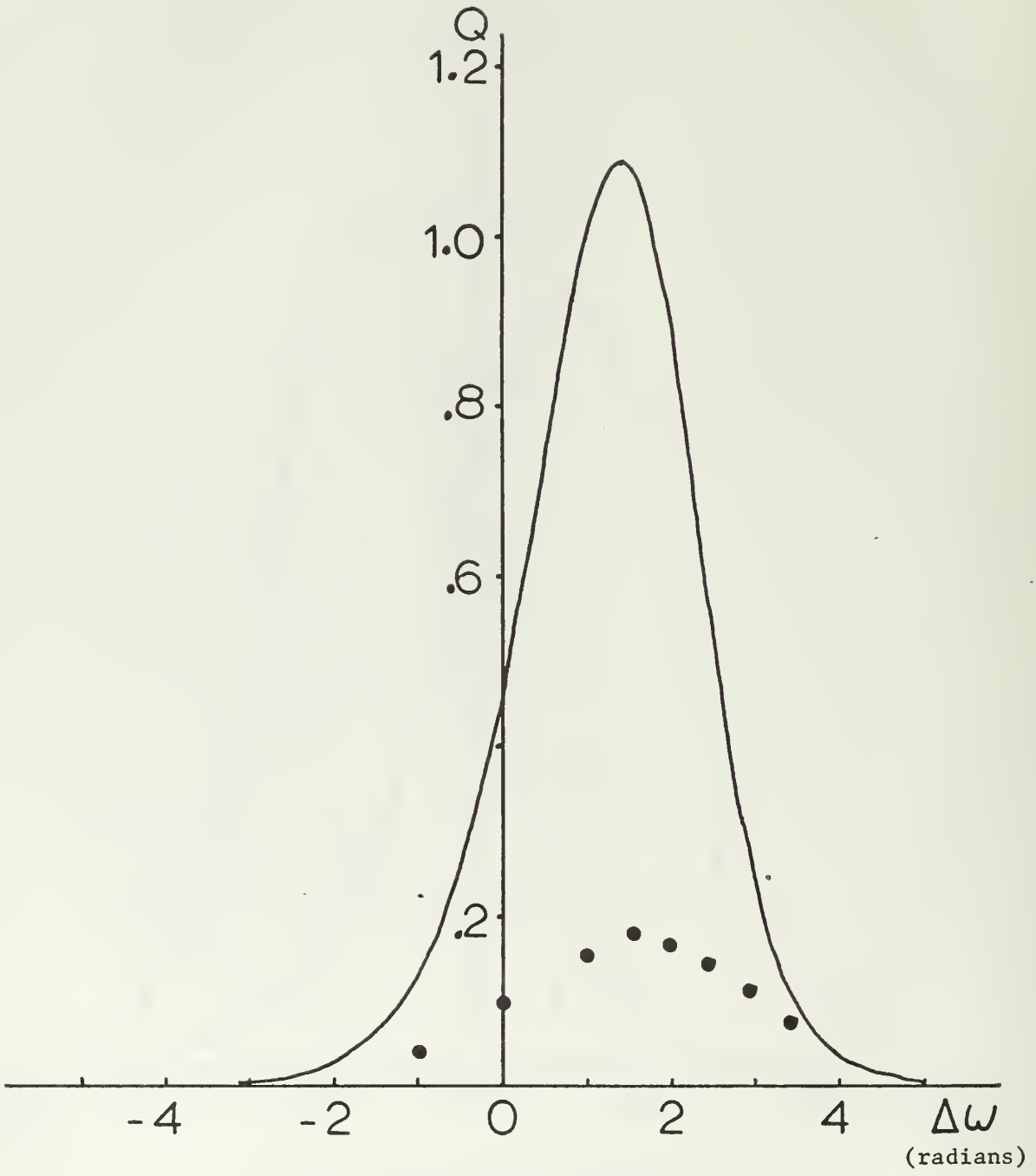

Q-curves of the Sixth Harmonic,
M = 0.009, SPL = 154 dB, L = 6'

Figure 26

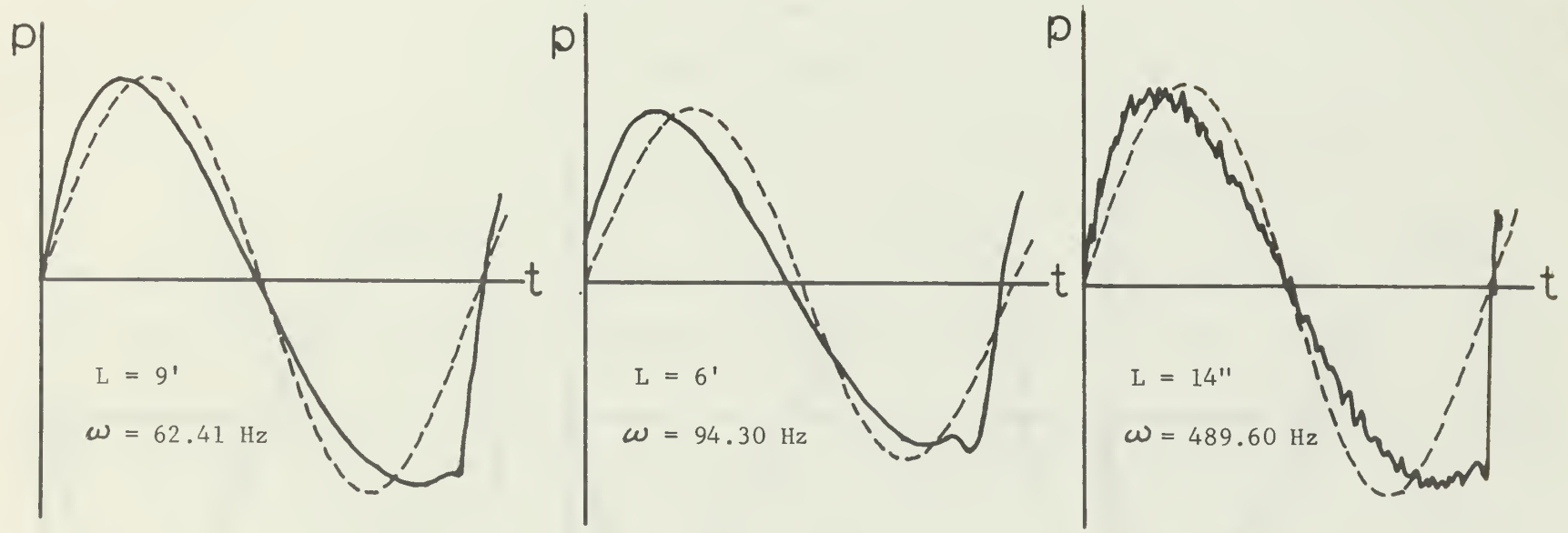

Pressure Waveforms

SPL = 155 dB, $\Delta\omega$ = 0, n = 1

Figure 27

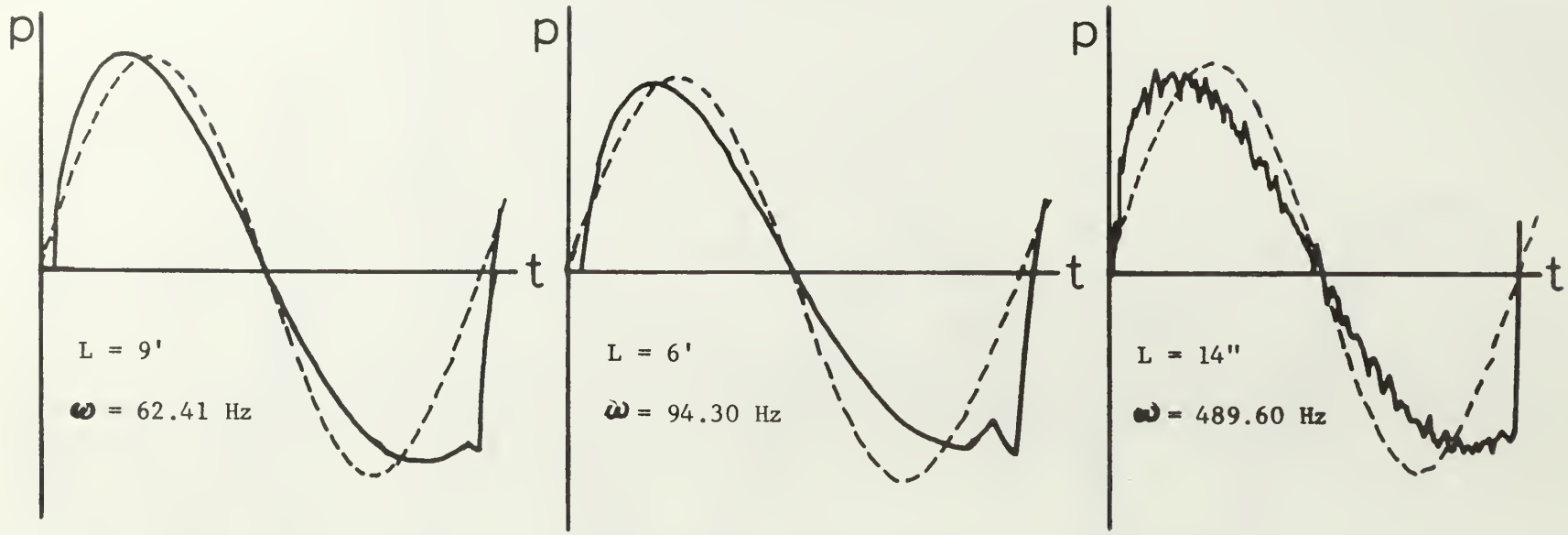

Pressure Waveforms

SPL = 157 dB, $\Delta\omega$ = 0, n = 1

Figure 18

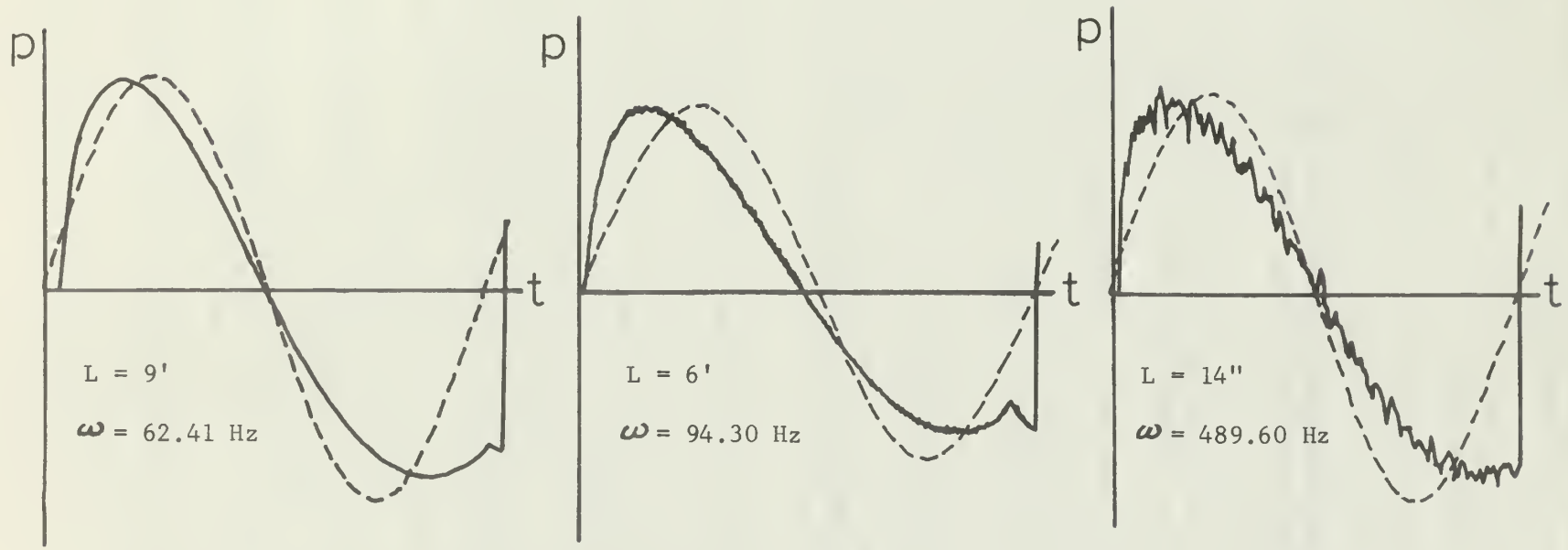

Pressure Waveforms

SPL = 160 dB, $\Delta\omega$ = 0, n = 1

Figure 29

BIBLIOGRAPHY

1. S. D. Poisson, "Memoire sur la Theorie du Son," J. de 1'Ecole Polytechnique, 7, 319-392 (1808).

2. Sir G. G. Stokes, "On a Difficulty in Theory of Sound," Phil. Mag. 23, 349-356 (1848).

3. G. B. Airy, Phil. Mag. 3, 34, 401 (1849).

4. B. Riemann, "Uber die Fortpflanzung ebener Luftwellen von endlicher Schwingungsweite", Gott Abh. 8, (Math), 43-65 (1858/9); Gesammelte Mathematische Werke, (Dover Publications, Inc., New York, 1953), 2nd Ed.

5. Rev. S. Earnshaw, "On the Mathematical Theory of Sound," Phil. Tran. Roy. Soc. London 150, 133-148 (1860).

6. G. Kirchhoff, Ann. Phys. Leipzig 134, 177-193 (1868).

7. Lord Rayleigh, Theory of Sound (Dover Publications, Inc., New York, 1945), 2nd Ed., Vols. 1 and 2.

8. R. D. Fay, "Plane Sound Waves of Finite Amplitude," J. Acoust. Soc. Am. 3, 222-241 (1931).

9. A. L. Thuras, R. T. Jenkins, and H. T. O'Neil, "Extraneous Frequencies Generated in Air Carrying Intense Sound Waves," J. Acoust. Soc. Am. 6, 173-180 (1935).

10. F. E. Fox and W. A. Wallace, "Absorption of Finite Amplitude Sound Waves," J. Acoust. Soc. Am. 26, 994-1006 (1954).

11. W. W. Lester, "On The Theory of the Propagation of Plane Finite Amplitude Waves in a Dissipative Fluid," J. Acoust. Soc. Am. 33, 1196-1199 (1961).

12. W. W. Lester, "A Theoretical and Experimental Study of the Propagation of Plane Finite Amplitude Waves in Real Fluids," Ultrasonics Laboratory, Michigan State University (1965).

13. Z. A. Gol'dberg, Akuct. Zhur. 2, 325 (1956) (English Trans.: Sov. Phys. - Acoust. 2, 346 (1956)).

14. Z. A. Gol'dberg, Akust. Zhur. 3, 149 (1957) (English Trans.: Sov. Phys. - Acoust. 3, 157 (1957)).

15. W. Keck and R. T. Beyer, "Frequency Spectrum of Finite Amplitude Ultrasonic Waves in Liquids," Phys. Fluids 3, 346-352 (1960).

16. N. N. Andreev, Akust. Zhur. 1, 2 (1955) (English Trans.: Sov. Phys. - Acoust 1, 2 (1955)).

17. I. Rudnick and R. W. Leonard, "The Attenuation of Repeated Shock Waves," J. Acoust. Soc. Am. 24, 456 (1952).

18. I. Rudnick, "On the Attenuation of a Repeated Sawtooth Shock Wave," J. Acoust. Soc. Am. 25, 1012-1013 (1953).

19. I. Rudnick, "On the Attenuation of Finite Amplitude Waves in a Liquid," J. Acoust. Soc. Am. 30, 564-567 (1958).

20. B. D. Cook, "New Procedure for Computing Finite-Amplitude Distortion," J. Acoust. Soc. Am. 34, 941-946 (1962).

21. D. T. Blackstock, "Convergence of the Keck-Beyer Perturbation Solution for Plane Waves of Finite Amplitude in a Viscous Fluid," J. Acoust. Soc. Am. 39, 411-413 (L) (1966).

22. J. B. Keller, "Finite Amplitude Sound Produced by a Piston in a Closed Tube," J. Acoust. Soc. Am. 26, 253-254 (L) (1954).

23. R. Betchov, "Nonlinear Oscillations of a Column of Gas," Phys. Fluids 1, 205-212 (1958).

24. R. A. Saenger and G. E. Hudson, "Periodic Shock Waves in Resonating Gas Columns," J. Acoust. Soc. Am. 32, 961-970 (1960).

25. W. Chester, "Resonant Oscillations in Closed Tubes," Graduate Aeronautical Laboratories, California Institute of Technology (N.D.).

26. A. B. Coppens and J. V. Sanders, "Finite-Amplitude Standing Waves in Rigid-Walled Tubes," J. Acoust. Soc. Am. (to be published March 1968).

27. P. G. Ruff, III, "Finite Amplitude Standing Waves in Rigid Walled Cavities," Thesis, Naval Postgraduate School, Monterey, California (1967)

28. L. E. Hargrove, "Fourier Series for the Finite Amplitude Sound Waveform in a Dissipationless Medium," J. Acoust. Soc. Am. 32, 511-512 (L) (1960).

29. D. E. Weston, "The Theory of the Propagation of Plane Sound Waves in Tubes," Proc. Phys. Soc. (London) B66, 695-709 (1953).

30. H. Helmholtz, Verhandlungen des Naturhistorishmedizischen Vereins zu Heidelberg 3, 16 (1863).

31. W. P. Mason, "The Propagation Characteristics of Sound Tubes and Acoustic Filters," Phys. Rev. 31, 283-295 (1928).

32. P. S. H. Henry, "The Tube Effect in Sound-Velocity Measurements," Proc. Phys. Soc. (London) 43, 341 (1931).

33. G. A. Norton, "Velocity of High Frequency Sound in Small Tubes," J. Acoust. Soc. Am. 7, 16-26 (1935).

34. R. D. Ray, "Attenuation of Sound in Tubes," J. Acoust. Soc. Am. 12, 62-67 (1940).

35. F. A. Angona, "Apparatus and Procedure for Measuring the Absorption of Sound in Gases by the Tube Method," J. Acoust. Soc. Am. 25, 1111-1116 (1953).

36. F. A. Angona, "Attenuation of Sound in a Tube," J. Acoust. Soc. Am. 25, 336 (L) (1953).

37. D. E. Weston and S. D. Campbell, "Experiments on the Propagation of Plane Sound Waves in Tubes," Proc. Phys. Soc. (London) B66, 769 (1953).

38. G. T. Kemp and A. W. Nolle, "The Attenuation of Sound in Small Tubes," J. Acoust. Soc. Am. 25, 1803 (1953).

39. L. E. Lawley, "The Propagation of Sound Through Gases Contained in Narrow Tubes," Proc. Phys. Soc. (London) B65, 181 (1952).

40. L. E. Lawley, "The Absorption of Sound in Carbon Dioxide Contained in Narrow Tubes," Proc. Phys. Soc. (London) B67, 65 (1954).

41. F. D. Shields and R. T. Lagemann, "Tube Corrections in the Study of Sound Absorption," J. Acoust. Soc. Am. 29, 470 (1957).

42. F. D. Shields, "Sound Absorption in Halogen Gases," J. Acoust. Soc. Am. 32, 180-185 (1960).

43. Bu. Standards Circular-564, Tables of Thermodynamic and Transport Properties of Air, etc., U. S. Government Printing Office, Washington, 20402 (1960).

44. F. D. Shields, K. P. Lee, and W. J. Wiley, "Numerical Solution for Sound Velocity and Absorption in Cylindrical Tubes," J. Acoust. Soc. Am. 37, 724-729 (1965).

45. F. A. Smith and W. Tempest, "Low Frequency Sound Propagation in Gases," J. Acoust. Soc. Am. 33, 1626 (1961).

46. J. G. Parker, "Effect of Several Light Molecules on the Vibrational Relaxation Time of Oxygen," J. Chem. Phys. 34, 1763-1772 (1961).

47. M. C. Henderson and G. J. Donnelly, "Acoustic Resonance Tube for High Pressure and Low f/P," J. Acoust. Soc. Am. 34, 779-784 (1962).

48. C. M. Harris, "Absorption of Sound in Air in the Audio-Frequency Range," J. Acoust. Soc. Am. 35, 11-17 (1963).

49. R. G. Harlow and R. Kitching, "Absorption of Sound in Mixtures of Oxygen and Water Vapor," J. Acoust. Soc. Am. 36, 1100-1103 (1964).

INITIAL DISTRIBUTION LIST

		No. Copies
1.	Defense Documentation Center Cameron Station Alexandria, Virginia 22314	20
2.	Library Naval Postgraduate School Monterey, California 93940	2
3.	Chief of Naval Research Office of Naval Research Washington, D. C. 20360	1
4.	Commander Naval Ships Systems Command Headquarters Washington, D. C. 20360	1
5.	Professor James V. Sanders Department of Physics Naval Postgraduate School Monterey, California 93940	7
6.	CDR Wayne "L" Beech 1108 Leahy Road Monterey, California 93940	2
7.	LT Paul G. Ruff, III USS Dale (DLG-19) FPO San Francisco, California 96627	1

DOCUMENT CONTROL DATA - R&D

(Security classification of title, body of abstract and indexing annotation must be entered when the overall report is classified)

1. ORIGINATING ACTIVITY *(Corporate author)* Naval Postgraduate School Monterey, California 93940	2a. REPORT SECURITY CLASSIFICATION Unclassified 2b. GROUP N/A

3. REPORT TITLE
Finite-Amplitude Standing Waves in Rigid-Walled Tubes

4. DESCRIPTIVE NOTES *(Type of report and inclusive dates)*
Thesis

5. AUTHOR(S) *(Last name, first name, initial)*
BEECH, Wayne "L", CDR, USN

6. REPORT DATE	7a. TOTAL NO. OF PAGES	7b. NO. OF REFS
December 1967	80	49

8a. CONTRACT OR GRANT NO. b. PROJECT NO. N/A c. d.	9a. ORIGINATOR'S REPORT NUMBER(S) N/A 9b. OTHER REPORT NO(S) *(Any other numbers that may be assigned this report)* None

10. AVAILABILITY/LIMITATION NOTICES
[redacted]

11. SUPPLEMENTARY NOTES None	12. SPONSORING MILITARY ACTIVITY Naval Ships System Command Washington, D. C. 20360

13. ABSTRACT

Finite-amplitude standing wave effects in air at ambient conditions contained in rigid-walled cylindrical tubes with large length to diameter ratios were experimentally investigated. These results were compared to a perturbation solution of one-dimensional non-linear acoustic wave equation which incorporates the dissipative effects due to viscous and thermal energy losses at the walls. The lowest resonance frequencies of the tubes ranged from 62.5 Hz to 1 kHz, and sound pressure levels (based on the fundamental) ranged up to 160 dB. The finite-amplitude distortion was in excellent agreement almost up to the onset of shock. A detailed investigation of small amplitude attenuation in standing wave tubes was conducted and compared with the Kirchhoff equations. Agreement within one percent was obtained when consideration was given to the numerical analysis correction and end-effect losses.

14 KEY WORDS	LINK A		LINK B		LINK C	
	ROLE	WT	ROLE	WT	ROLE	WT
Attenuation Constant						
Attenuation Coefficient						
End-Effect Losses						
Finite-Amplitude						
Non-Linear Acoustic Wave Equation						
Perturbation Solution						
Q-curves						
Resonance Tubes						
Rigid-Walled Tubes						
Standing Waves						